Science of the Total Environment 730 (2020) 138899

Contents lists available at ScienceDirect

Science of the Total Environment

journal homepage: www.elsevier.com/locate/scitotenv

Airborne bacteria structure and chemical composition relationships in winter and spring PM10 samples over southeastern Italy

S. Romano [a,*], S. Becagli [b], F. Lucarelli [c], G. Rispoli [a], M.R. Perrone [a]

[a] Department of Mathematics and Physics, University of Salento, Via per Arnesano, 73100 Lecce, Italy
[b] Department of Chemistry, University of Florence, Via della Lastruccia 3, 50019, Sesto Fiorentino, Florence, Italy
[c] Department of Physics, University of Florence and I.N.F.N. (Unit of Florence), Via Sansone, 50019, Sesto Fiorentino, Florence, Italy

HIGHLIGHTS

- Chemical species and airborne bacteria abundance relationships are season-dependent
- Correlation coefficients and RDA are used to study bacterium-chemical relations
- Spearman coefficients show good evidence of relations between bacteria and chemicals
- *Proteobacteria* phylum does not show significant correlations with chemical species
- Chemical species/pollution sources likely affect the bacterial community structure

GRAPHICAL ABSTRACT

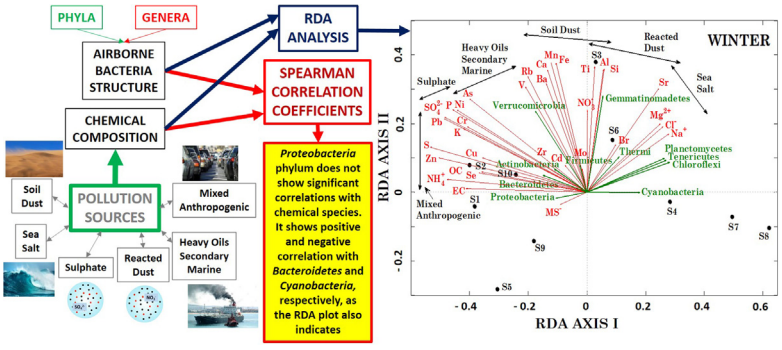

ARTICLE INFO

Article history:
Received 20 January 2020
Received in revised form 18 April 2020
Accepted 20 April 2020
Available online 28 April 2020

Editor: Jianmin Chen

Keywords:
Airborne bacteria structure
PM10 chemical species
Spearman correlation coefficients
Redundancy discrimination analysis
Bacterial community shaping
Seasonal dependence analyses

ABSTRACT

The Redundancy Discrimination Analysis (RDA) and Spearman correlation coefficients were used to investigate relationships between airborne bacteria at the phylum and genus level and chemical species in winter and spring PM10 samples over Southeastern Italy. The identification of main chemical species/pollution sources that were related to and likely affected the bacterial community structure was the main goal of this work. The 16S rRNA gene metabarcoding approach was used to characterize airborne bacteria. Seventeen phyla and seventy-nine genera contributing each by mean within-sample relative abundance percentage > 0.01% were identified in PM10 samples, which were chemically characterized for 33 species, including ions, metals, OC, and EC (organic and elemental carbon, respectively). Chemical species were associated with six different pollution sources. A shift from winter to spring in both bacterial community structure and chemical species mass concentrations/sources and the relationships between them was observed. RDA triplots pointed out significant correlations for all tested bacterial phyla (genera) with other phyla (genera) and/or with chemical species, in contrast to correlation coefficient results, which showed that few phyla (genera) were significantly correlated with chemical species. More specifically, in winter *Bacillus* and *Chryseobacterium* were the only genera significantly correlated with chemical species likely associated with particles from soil-dust and anthropogenic pollution source, respectively. In spring, *Enterobacter* and *Sphingomonas* were the only genera significantly correlated with chemical species likely associated with particles from the anthropogenic pollution and the marine and soil-dust sources, respectively. The results of this study also showed that the correlation coefficients were the best tool to obtain unequivocal identifications of the correlations of phyla (genera) with chemical species. The seasonal changes of the PM10 chemical composition, the microbial community structure, and their relationships suggested that the seasonal

* Corresponding author at: Department of Mathematics and Physics "E. De Giorgi", University of Salento, Via per Arnesano, 73100 Lecce, Italy.
E-mail address: salvatore.romano@unisalento.it (S. Romano).

https://doi.org/10.1016/j.scitotenv.2020.138899

changes of atmospheric particles may have likely contributed to seasonal changes of bacterial community in the atmosphere.

1. Introduction

The atmospheric particulate matter (PM) is a complex and dynamic mixture containing various abiotic and biotic particles. Many studies addressed the PM potential influences on the atmospheric and terrestrial ecosystems (e.g., Seinfeld and Pandis, 1998; Fröhlich-Nowoisky et al., 2016; Estillore et al., 2016; Mayol et al., 2017; Zhong et al., 2019). Microorganisms represent about 10% of the total aerosol particles, according to Wei et al. (2015). In particular, airborne bacteria with abundance from 10^5 to 10^6 cells m^{-3} in near surface atmosphere may account for >80% in PM10 particles (Cao et al., 2014). Mayol et al. (2017) indicated that the microbial abundance in the atmospheric boundary layer over the open ocean can range from $1 \cdot 10^2$ to $1.8 \cdot 10^5$ cells m^{-3} depending on the sampling location. Estimations of the marine microbial abundance related to a specific area were reported over the North Atlantic Ocean (Mayol et al., 2014), over the Southeastern Mediterranean Sea (Rahav et al., 2019; Mescioglu et al., 2019a), and over the Red Sea (Mescioglu et al., 2019b; Yahya et al., 2019). Airborne bacteria may be suspended as individual cells or found as agglomerate of many bacterial cells. More likely, they are attached to abiotic particles, such as soil, against harsh atmospheric conditions (i.e., high UV intensity, low nutrient concentration, and humidity) for survival and growth (Yan et al., 2018; Zhong et al., 2019). Therefore, the atmosphere may play a significant role in feeding the microbial activity and growth. In fact, the atmosphere represents the main transport vector of aerosols, in particular mineral dust and anthropogenic constituents, which also supply nutrients to the ocean and land surface (e.g., Rahav et al., 2019; Mackey et al., 2012). However, besides acting as carriers and supplying the nutrition, abiotic airborne particles may also inactivate bacteria (e.g., Yan et al., 2018; Zhai et al., 2018) and alter the bacterial community structure. As mentioned, bacteria are highly sensitive to nutrient availability, concentrations of pollutants (Estillore et al., 2016), and altered environmental conditions (e.g., Jordaan and Bezuidenhout, 2016). Moreover, after their deposition, abiotic particles may have a variety of effects on the airborne bacterial diversity and richness (Yan et al., 2018). In fact, the airborne microorganisms attached to abiotic particles can gradually form many abundant and mutable communities generating microbial diversity over PM (Zhai et al., 2018). Rahav et al. (2016, 2018a, 2018b) investigated the potential impacts of airborne microbes upon deposition into marine ecosystems. They pointed out that the aerosol deposition could supply a high diversity of airborne microbes, which in turn can affect the surface microbial composition and biological production. Reche et al. (2018) found that the deposition rates of bacteria increased during rain events and Saharan dust intrusion in the Sierra Nevada Mountains (Spain). They used a platform located above the atmospheric boundary layer to reduce anthropogenic aerosol effects. Similar results were also found by Peter et al. (2014) during rain events and Saharan dust outbreaks at a mountain lake in the Austrian Alps. Therefore, precipitations could also represent significant pathways by which airborne microbes fall to the ground surface affecting the bacterial community. In fact, Hiraoka et al. (2017) found that precipitations affected the microbial communities with specific seasonal variations and habitats (animal-, soil-, and marine-associated environments) in the Greater Tokyo Area (Japan).

Bacteria with a size range of 1.1 to 2.1 μm can reside in the air for several days (Raisi et al., 2013) and can be transported over long distances before removal from the atmosphere by precipitation or direct deposition onto surfaces (e.g., Gat et al., 2017; Romano et al., 2019a). Mayol et al. (2017) estimated that the atmospheric transport of microbes over the oceans might play a major role in the dispersal of surface marine microbes as well as in the intercontinental transport of their terrestrial counterparts. In fact, sea spray is also an important contributor of airborne microbes, as proved by Sharoni et al. (2015) over the North Atlantic and Yahya et al. (2019) over the Red Sea.

Recent developments of culture-independent methods for microbiological analysis have opened up the possibility to extensively study and characterize the atmospheric microbiome through, as an example, the applications of DNA-based methods (Fröhlich-Nowoisky et al., 2016). Consequently, more accurate analyses on the diversity and community composition of PM-associated airborne bacteria have been performed worldwide (Barberán et al., 2015; Innocente et al., 2017; Gat et al., 2017; Yan et al., 2018; Pan et al., 2019; Romano et al., 2019a). Most of the previous studies focused on the impact of meteorological parameters (relative humidity, wind direction, wind speed, and temperature) and gaseous components (NO_2, SO_2, O_3, and CO) on the bacterial diversity and structure (Zhen et al., 2017; Guo et al., 2018; Yan et al., 2018; Li et al., 2018; Pan et al., 2019). Estillore et al. (2016) investigated the reactivity of aerosol particles of biological origin with some oxidant species (OH, NO_3, and O_3) present in the atmosphere. Gat et al. (2017) and Polymenakou et al. (2008) investigated the impact of long-range transported air masses associated with dust storms of different origin (North Africa, Syria, and Saudi Arabia) on the airborne microbiome of Mediterranean sites. Herut et al. (2016) analyzed the potential impact of both long-range transported Saharan dust and polluted aerosol on the microbial populations over the Eastern Mediterranean Sea. Several works proved that the air mass pathways can affect the richness and the diversity of the airborne bacterial community (e.g., Kellogg and Griffin, 2006; Katra et al., 2014; Rahav et al., 2016). Romano et al. (2019a) investigated the role of meteorological parameters and long-range transported air masses on the airborne bacterial structure of PM10 samples collected both in winter and in spring in Lecce (Southeastern Italy). They showed that the richness and biodiversity of the PM10 bacterial community on average increased from winter to spring, while the sample dissimilarity presented an opposite trend since it decreased from winter to spring. The spring meteorological conditions over the Mediterranean could have contributed to the above results. In fact, the spring decrease of rainy days over the Mediterranean likely contributed to maintain for longer time the bacterial community in the atmosphere and favoured the mixing of particles from different sources (Perrone et al., 2019a).

The relationships between the bacterial community structure and the chemical composition of PM samples have recently been investigated at Chinese sites (Beijing, Guilin) during haze and non-haze days (Sun et al., 2018; Guo et al., 2018; Zhong et al., 2019), and over northern Italy (Innocente et al., 2017) and the Mediterranean Sea (Mescioglu et al., 2019a). They found that some chemical species probably contributed to the shaping of bacterial community structure. In particular, Sun et al. (2018) highlighted that chemical constituents in PM were closely associated with microbes as they were the survival environment of microorganisms. The great importance of investigating the impact of meteorological parameters, atmospheric pollutants, oxidants, and PM chemical species on the bacterial community structure is justified by the need of improving the understanding of the bacterial structure survival and changes. On the other end, changes on the bacterial diversity can affect the functional dynamics of the whole ecosystem by altering the ecosystem processes (physical, chemical, and biological) through metabolic feedbacks (e.g., Zhai et al., 2018).

The relationships between the airborne bacterial structure and the chemical composition in winter and spring PM10 samples were investigated in this study, to contribute to the studies on the relationships

between chemical species and bacterial structure and their seasonal dependence. We believe that strong relationships between bacteria and chemical species could also indicate if atmospheric chemical species and their seasonal changes have likely contributed to the seasonal changes of the bacterial community in the atmosphere, as stated in previous studies. We are aware that laboratories studies in controlled air conditions could represent a good tool to investigate the relationships between atmospheric particles and bacteria structure. Nevertheless, field experiments are complementary and scientifically important, since laboratory experiments may not exactly reproduce "real" atmospheric conditions. Preliminary results on the PM10 samples analyzed in this study were already reported in Romano et al. (2019a). They investigated the impact of meteorological parameters and long-range-transported air masses on the bacterial community structure. In contrast, the relationships between the airborne bacteria structure and the PM10 chemical composition as well as their seasonal dependence have been investigated in this study, as mentioned. We are aware that the chemical composition of the monitored atmospheric particles was also affected by the long-range-transported air masses. However, the impact of long-range advected air masses on the chemical composition of the particulate matter at the study site depends not only on the air mass source, but also on the advection route followed by the air masses before reaching the study site and the study site characteristics. Consequently, chemical species were linked to pollution sources to also show their role on the bacteria structure.

Moreover, analytical techniques different from the ones in Romano et al. (2019a) have been used in this study to investigate the relations between the airborne bacteria structure and the PM10 chemical composition in winter and spring. Therefore, the main topic of this study is different than the one of the previous paper and the results will be complementary to the ones reported by Romano et al. (2019a). More specifically, the Spearman correlation coefficients have been compared with the main outcomes from the Redundancy Discriminant Analysis (RDA), to also highlight benefits and limits of the two methodologies. RDA is a widespread technique to study biological data coupled to environmental data. Several factors affect the microbial community shaping and, therefore, different statistical methodologies are commonly used to better highlight the role of each factor.

The PM10 samples were collected at a coastal site of the Central Mediterranean basin away from large sources of local pollution. In fact, due to its particular geographical location, the study site is affected by a large variety of aerosol types, mainly desert dust from the Sahara desert, polluted particles from Northern and Eastern Europe, sea spray from the Mediterranean Sea itself or from the Atlantic Ocean, and biomass burning particles from forest fires. All these factors highlight the importance of investigating main features of the aerosol microbiome over the Mediterranean basin.

2. Material and methods

2.1. Sample collection

The PM10 samples were collected at about 10 m above the ground level, on the roof of the Mathematics and Physics Department of the University of Salento, which is located in a suburban site (40.3°N; 18.1°E) of Southeastern Italy. The study site is representative of coastal sites of the Central Mediterranean, away from large sources of local pollution. A detailed description of the study site's main features can be found in Perrone et al. (2014, 2015).

Different PM10 samplers operating at 2.3 $m^3\ h^{-1}$ were used to simultaneously collect PM10 particles on different filters for chemical analyses and the recovery of bacteria. The dataset of this study is based on 10 winter samples (detected from January to March 2018) and 10 spring samples (from May to June 2018). Table S1 of the Supplementary Material shows the PM10 and chemical species mass concentrations of all the analyzed samples in addition to the sampling date and time (72 and 48 h for winter and spring samples, respectively). Main statistical data for the measured parameters (PM10 and chemical species mass concentrations), including means, standard deviations (SDs), medians, minima and maxima values, 25th and 75th percentiles, skewness, and data representativeness (REPR) have also been reported in Table S1. PM10 particles were collected on 47-mm-diameter quartz filters to determine the mass concentration of ion species (Na^+, NH_4^+, Mg^{2+}, Cl^-, NO_3^-, SO_4^{2-}, and MS^-) and elemental and organic carbon (EC and OC, respectively). PM10 particles were also simultaneously collected on two different 47-mm-diameter polytetrafluoroethylene (PTFE) filters (TEFLO W/RING 2 μ from VWR International S.R.L.) to determine metal (As, Ba, Cd, Cr, Mo, Ni, Pb, V, Al, Si, K, Ca, Ti, Mn, Fe, Cu, Zn, Rb, Sr, and Zr) and Br, P, S, and Se mass concentrations and characterize the bacterial community. Burton et al. (2007) proved that PTFE filters are highly efficient for collecting sub-micrometer and nano-scale aerosol particles, including bacteria and viruses. After sampling, each filter was put in a sterile box and stored at −20 °C, since the bacterial growth was unlike at such temperature, according to Mykytczuk et al. (2012). Two control filters, which were not subjected to sampling, but handled and stored in accordance with the same procedure applied to sampled filters, were used as negative control. The operator used masks and sterile tweezers during sampling to minimize the contamination risks.

2.2. Analyses of chemical components

Ion chromatography analyses were performed at the Chemistry Department of the University of Florence by Flow Analysis Ion Chromatography (FA-IC, modified after Morganti et al., 2007) to determine the mass concentrations of selected anions (Cl^-, NO_3^-, SO_4^{2-}, and MS^-) and cations (Na^+, NH_4^+, and Mg^{2+}) in the PM10 samples. Particular attention was devoted to the evaluation of the blanks, which was at least one order of magnitude lower than the mean concentration found in the analyzed samples for each reported ion result. More details about ion and metal analyses can be found in Becagli et al. (2012).

The total (soluble and insoluble) elemental composition (As, Ba, Cd, Cr, Mo, Ni, Pb, V, Al, Si, P, S, K, Ca, Ti, Mn, Fe, Cu, Zn, Se, Br, Rb, Sr, and Zr) in each PM10 sample was determined by the particle induced X-ray emission (PIXE) technique at the LABEC I.N.F.N. (Istituto Nazionale di Fisica Nucleare) laboratory in Florence, Italy (Lucarelli et al., 2011).

The thermal optical transmittance technique by means of the Sunset Carbon Analyzer Instrument (Birch and Cary, 1996) was used to determine EC and OC mass concentrations in a 1.5 cm^2 punch of the PM10 filter sample by the EUSAAR-2 temperature program protocol (Cavalli et al., 2010). Measurement uncertainties were of 10% and 6% for EC and OC, respectively. The OC and EC analyses were performed at the Mathematics and Physics Department of the University of Salento. More details can be found in Perrone et al. (2009).

The mean values of PM10 and corresponding chemical species mass concentrations ± standard error of the mean (SEM) for the 10 samples collected in winter (W, January–March) and the 10 samples collected in spring (S, May–June) have been reported in Table 1. Mean mass percentages with respect to the total sampled PM10 mass have also been reported in brackets. An overview of the chemical species mass percentages in the 20 PM10 samples is shown in Fig. S1 of the Supplementary Material.

2.3. DNA extraction and data analysis

A detailed description of the used methodology to recover bacteria and debris from PM10 filters and extract DNA is provided in Romano et al. (2019a). The DNA samples were subjected to the sequencing of the V3 and V4 region of the 16S rRNA gene, PCR amplifications, and taxonomic classification. A total of 7,317,407 reads was assigned to 1738 OTUs (with >0.01% within-sample relative abundance) at the threshold of 97% sequence similarity (Edgar, 2013).

Table 1
Mean values of PM10 and corresponding chemical species mass concentrations ± standard error of the mean (SEM), for the 10 samples collected in winter (W, January–March) and the 10 samples collected in spring (S, May–June). The mean mass percentages of the analyzed chemical species with respect to the total sampled mass are reported in brackets.

Species ($\mu g\ m^{-3}$)	Winter		Spring	
	Mean	SEM	Mean	SEM
PM10	23.9	2.6	21.8	1.8
OC	5.4 (22.6)	1.1	3.8 (17.4)	0.4
EC	1.3 (5.4)	0.2	0.9 (4.1)	0.1
Na^+	1.4 (5.9)	0.3	0.6 (2.8)	0.1
NH_4^+	0.4 (1.7)	0.1	1.0 (4.6)	0.2
Mg^{2+}	0.19 (0.8)	0.04	0.12 (0.6)	0.01
Cl^-	1.7 (7.1)	0.5	0.3 (1.4)	0.1
NO_3^-	1.6 (6.7)	0.2	0.9 (4.1)	0.1
SO_4^{2-}	2.4 (10.0)	0.3	4.4 (20.2)	0.7
MS^-	0.005 (0.02)	0.001	0.042 (0.2)	0.007
As	0.0003 (0.001)	0.0001	0.0028 (0.01)	0.0009
Ba	0.007 (0.03)	0.001	0.009 (0.04)	0.002
Cd	0.0001 (0.0004)	0.0001	0.0001 (0.0004)	0.0001
Cr	0.0014 (0.01)	0.0003	0.0023 (0.01)	0.0007
Mo	0.0007 (0.003)	0.0001	0.0023 (0.01)	0.0004
Ni	0.0011 (0.005)	0.0002	0.0025 (0.01)	0.0005
Pb	0.0032 (0.01)	0.0007	0.0027 (0.01)	0.0006
V	0.0023 (0.01)	0.0004	0.0071 (0.03)	0.0009
Al	0.17 (0.7)	0.08	0.30 (1.4)	0.06
Si	0.4 (1.7)	0.2	0.7 (3.2)	0.1
P	0.009 (0.04)	0.001	0.028 (0.1)	0.004
S	0.7 (2.9)	0.1	1.3 (6.0)	0.2
K	0.41 (1.7)	0.07	0.25 (1.1)	0.02
Ca	0.47 (2.0)	0.09	0.76 (3.5)	0.09
Ti	0.013 (0.05)	0.006	0.019 (0.1)	0.003
Mn	0.0041 (0.02)	0.0008	0.0062 (0.03)	0.0007
Fe	0.27 (1.1)	0.06	0.31 (1.4)	0.04
Cu	0.004 (0.02)	0.001	0.005 (0.02)	0.001
Zn	0.011 (0.05)	0.002	0.014 (0.1)	0.002
Se	0.0004 (0.002)	0.0001	0.0006 (0.003)	0.0001
Br	0.0080 (0.03)	0.0009	0.0041 (0.02)	0.0001
Rb	0.0013 (0.005)	0.0005	0.0010 (0.005)	0.0002
Sr	0.0019 (0.01)	0.0006	0.0022 (0.01)	0.0003
Zr	0.0009 (0.004)	0.0001	0.0012 (0.006)	0.0003

The rarefaction curves for the 10 winter (solid lines) and spring (dashed lines) samples, estimating the number of observed bacterial OTUs at the 97% similarity level, have been reported in Fig. S2. A greater number of OTUs was associated on average with spring samples and the highest OTU number (995) was associated with sample S18 monitored on 13 June. The sample's beta diversity was characterized by the Bray-Curtis (BC) dissimilarity index (Ricotta and Podani, 2017).

2.4. Redundancy discriminant analysis

The Redundancy Discriminant Analysis (RDA) represents a widespread chemometric procedure to study biological data coupled to environmental data, as chemical species or meteorological parameters (e.g., Wang et al., 2012; Innocente et al., 2017). The RDA can be defined as the multivariate extension of simple linear regression that is applied to sets of variables (Van den Wollenberg, 1977). More specifically, a combination of two datasets is required to run RDA: "species data" that represent the response (or dependent) variables and "environmental variables" that indicate the explanatory (or predictive) variables (e.g., Paliy and Shankar, 2016).

In this work, the RDA technique was used to investigate the relationships between the bacterial RAs (both at the phylum and at the genus level) as "species data" and the chemical species mass concentrations as "environmental variables". Before applying the RDA procedure to the selected biological and chemical data, all the singletons were removed and the Hellinger transformation was applied to the phyla and genera RA data (e.g., Legendre and Gallagher, 2001; Paliy and Shankar, 2016). The RDA analysis was applied to the selected data by using the *Fathom Toolbox for MATLAB* (Jones, 2017). Chemical species data (considered as "environmental variable" for RDA) that best explained phyla and genera RAs were determined by Monte Carlo tests with 499 unrestricted permutations, as described by Innocente et al. (2017).

3. Results and discussion

3.1. PM10 and chemical species mass concentrations

PM10 and chemical species mass concentrations showed mean values larger than corresponding median values. Therefore, they were characterized by positive skewness values spanning the 0.24–4.46 range (Table S1), for which almost normal distributions (skewness close to zero) were observed. The representativeness of PM10 and chemical species mass concentrations of this study has been tested using the methodology proposed by Ganesan et al. (2016), which allowed calculating the representativeness parameter (denoted as REPR) reported in Table S1. REPR values close to zero indicate that the selected subset cannot represent the global dataset, while REPR values close to 1 indicate that subset and global dataset present a similar frequency distribution. REPR values have been estimated by comparing the PM10 and chemical species dataset of this study related to the year 2018 with the ones of the years 2012 (reported in Perrone et al., 2018) and 2015 (reported in Perrone et al., 2019a, 2019b; Romano et al., 2020; Pietrogrande et al., 2018). We have found that the REPR values calculated for the chemical species present in all the three analyzed datasets were all larger than 0.60. This last result proved that the dataset of PM10 and chemical species mass concentrations investigated in this study could be considered characterized by a high representativeness with respect to the selected global dataset. Therefore, they could be considered as representative of PM10 particles at the study site.

3.1.1. Seasonal dependence of PM10 and chemical species mass concentrations

The PM10 and chemical species mass concentrations were characterized by significant seasonal variations, as shown in Table 1. In fact, the mean PM10 mass concentration slightly decreases (~9%) from winter to spring. Analogously, the mass percentage of OC, EC, Na^+, Cl^-, and NO_3^- is greater in W than in S. Conversely, the mass percentage of NH_4^+, SO_4^{2-}, and almost all tested metals is greater in S than in W. The seasonal dependence of the ground-level PM properties at the study site has been highlighted in previous studies (e.g., Perrone et al., 2009, 2011, 2013a, 2015; Pietrogrande et al., 2018). In particular, a detailed discussion on the PM10 chemical speciation and seasonal dependence is provided in Perrone et al. (2018, 2019a). The enhanced photochemical processes and the low air mass replacement occurring in warm seasons over the Mediterranean basin (e.g., Querol et al., 2009), and therefore at the study site, contributed to the seasonal dependence of the PM properties. Warm seasons favour the air mass aging associated with local and/or long-range transported aerosols also because of the decrease of rainy days.

3.1.2. Association of chemical species with pollution sources

The association of chemical species with pollution sources has been reported in previous studies related to the study site (e.g., Perrone et al., 2019a; Romano et al., 2020). The Positive Matrix Factorization Technique (PMF) was applied to PM10 chemically speciated data to identify main pollution sources. According to Perrone et al. (2019a), six distinct pollution sources were identified by PMF, taking into account 23 chemical species including ions (Na^+, NH_4^+, K^+, Mg^{2+}, Ca^{2+}, Cl^-, NO_3^-, SO_4^{2-}, MS^-), metals (Al, Ba, Cr, Cu, Fe, Mn, Ni, Pb, Sr, Ti, V, Zn), OC, and EC, in addition to PM10 mass concentrations. Mixed Anthropogenic (MAN), Heavy Oil/Secondary Marine (OSM), Soil Dust (SDU), Reacted Dust (RDU), Sulphate (SUL), and Sea-Salt (SES) were the six identified pollution sources. The labelling of the MAN source was due to the presence of markers both from traffic (e.g., EC, OC, Cu, Fe, Ba) and from biomass-

Table 2
Main pollution sources and corresponding tracers at the study site (Lecce, Italy), according to Perrone et al. (2019a).

Pollution sources	Tracers (chemical species)
Sulphate (**SUL**)	SO_4^{2-}, NH_4^+, Pb
Heavy Oils / Secondary Marine (**OSM**)	V, Ni, MS^-, Ca
Mixed Anthropogenic (**MAN**)	EC, OC, Cu, Fe, Ba (traffic markers) K, OC, EC (biomass burning markers)
Soil Dust (**SDU**)	Ca, Al, Fe, Mn, Sr, Ti, Ba
Reacted Dust (**RDU**)	NO_3^-, Na^+, Mg^{2+}
Sea Salt (**SES**)	Na^+, Cl^-, Mg^{2+}, Sr

burning (e.g., K^+, OC, EC), according to Chow (1995) and Viana et al. (2008). The heavy oil/secondary marine source was characterized by high values of V and Ni, typical tracers of heavy oil combustion. Their contributions were likely due to pollution from ship emissions according to Becagli et al. (2012). Main tracers of the soil dust source were Ca^{2+}, Al, Fe, Mn, Sr, and Ti. The reacted dust source had signatures from crustal particles mixed with secondary species like nitrates and sulphates (Perrone et al., 2013b). SO_4^{2-}, NH_4^+, and Pb were the main tracers of the sulphate source. Main tracers of the sea salt source were Na^+, Cl^-, and Mg^{2+}, even if Sr, V, Zn, Al, Ca, and Fe could also have contributed, according to Chow (1995). Table 2 summarizes main pollution sources and corresponding tracers at the study site, according to Perrone et al. (2019a). The seasonal dependence of the identified pollution sources was also investigated by Perrone et al. (2019a). They showed that the percentage contribution of the MAN and SES sources decreased from Autumn-Winter to Spring-Summer. In contrast, the percentage contribution of the OSM, SDU, RDU, and SUL sources increased from Autumn-Winter to Spring-Summer.

3.2. Seasonal dependence of bacterial phyla and corresponding habitats

Seventeen predominant phyla contributing each by a mean within-sample relative abundance (RA) percentage > 0.01% were identified in the collected PM10 samples. Their overall RA was of 92.78%. Fig. 1 shows the phylum within-sample RA both in (a) winter (S1-S10) and in (b) spring (S11-S20) samples. *Proteobacteria*, *Cyanobacteria*, *Actinobacteria*, *Firmicutes*, and *Bacteroidetes* were the most abundant phyla and were found in all winter and spring samples (Fig. S3), with the exception of *Bacteroidetes*, which was not detected in sample S8 (Fig. 1a). Different studies related to the analysis of the microbial community diversity over the Eastern Mediterranean region showed results similar to those of this study, even if they were performed during the advection of desert dust (Mescioglu et al., 2019a). Gat et al. (2017) studied the bacterial community during dusty and dust-free days in Rehovot (Israel). They found that the samples monitored during advection of desert dust of different origin and during clear-sky days exhibited distinct features of the bacterial phyla diversity. Nevertheless, *Proteobacteria*, *Actinobacteria*, *Firmicutes*, and *Bacteroidetes* were found as the most abundant phyla. Mescioglu et al. (2019b) collected samples over the Northern Red Sea during a dust storm and found that *Proteobacteria*, *Actinobacteria*, *Firmicutes*, *Bacteroidetes*, and *Gemmatimonadetes* were the most abundant phyla. They also showed that the airborne microorganisms were viable after the deposition processes. Therefore, the airborne microbioma could have significantly impacted the

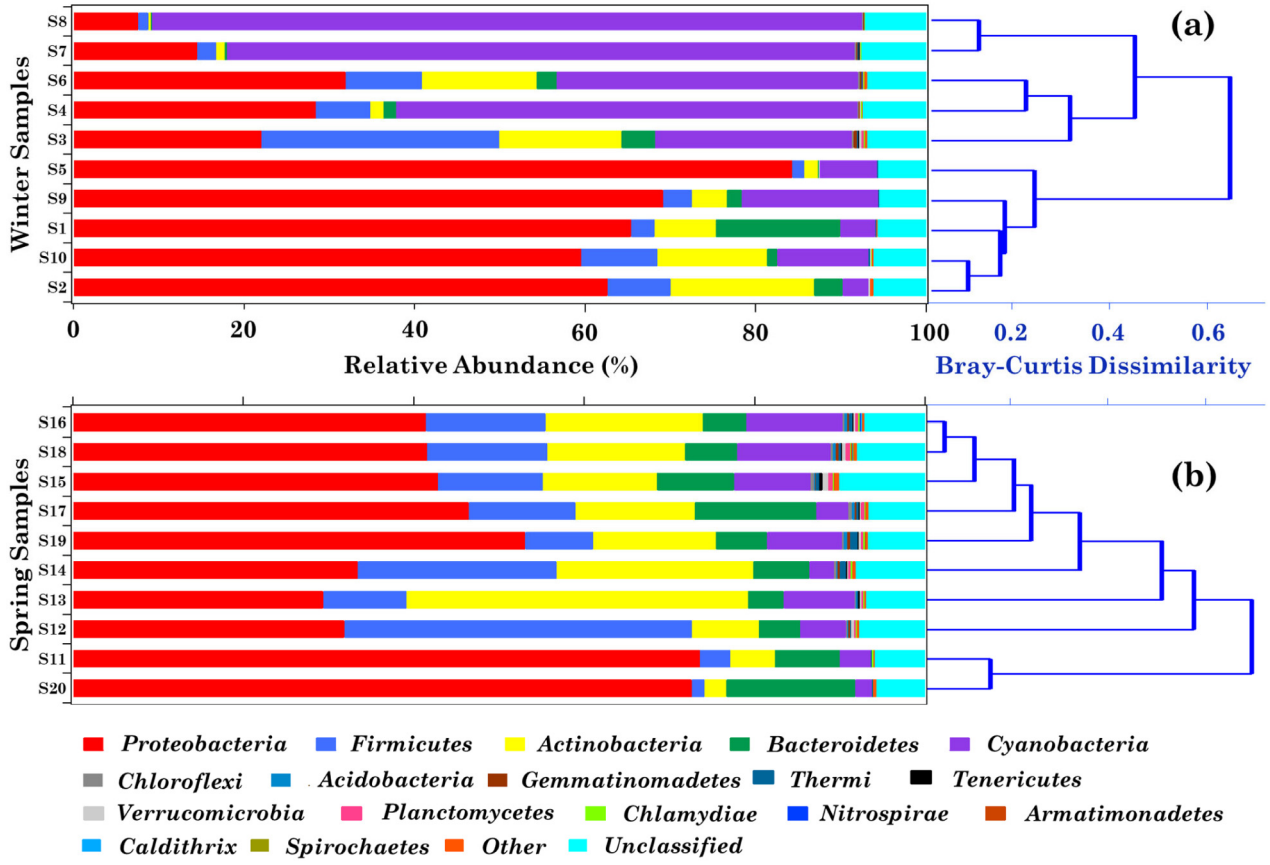

Fig. 1. Relative percentage contribution of the 17 most abundant (> 0.01% mean within-sample relative abundance) bacterial phyla in (a) winter and (b) spring samples. The <0.01% mean within-sample relative abundance and unclassified bacterial phyla have been denoted as "Other" and "Unclassified", respectively. Bray-Curtis dissimilarity dendrograms highlighting the relatedness of the phylum-level bacterial communities in (a) winter and (b) spring samples have also been reported.

biogeochemical processes in the arid regions where dust storm events occurred. Analyses on the bacterial community diversity over the Eastern Mediterranean region during intense dust outbreaks were also reported by Mazar et al. (2016), Katra et al. (2014), and Polymenakou et al. (2008). The results about the bacterial phyla diversity found at the study site are also consistent with those related to other areas, like China (e.g., Cao et al., 2014; Gao et al., 2017), United States (e.g., Barberán et al., 2015), and over tropical and subtropical oceans (Mayol et al., 2017). In fact, the above mentioned phyla could be found at relatively high abundance in various terrestrial and aquatic environment (TAE) habitats.

Fig. 1 shows that the within-sample relative abundance of each phylum varied from sample to sample. The Bray-Curtis dissimilarity dendrogram was also plotted in Fig. 1 to highlight the relatedness of the phylum bacterial communities among (a) winter and (b) spring samples. The related $B_{i,j}$ matrix based on the bacterial phylum RAs is shown in Table S2. Values close to zero indicate samples that share similar phylum RAs, while values close to 1 indicate samples that have different phylum RAs. Fig. 1a shows that winter samples could be grouped in two main clusters. One cluster consisted of samples S2, S10, S1, S9, and S5, being all characterized by *Proteobacteria* RAs >60% and $B_{i,j}$ values <0.20. The $B_{2,10}$ index value reached the smallest value (0.08), since samples S2 and S10 were characterized by a rather similar bacterial phylum structure. The high RA of *Firmicutes* characterized the other winter cluster that consisted of samples S3, S4, S6, S7, and S8. The dissimilarity index between the two W clusters (0.65) indicates a clear and significant difference among them (Fig. 1a). The BC dissimilarity dendrogram of the spring samples allowed identifying the cluster composed by samples S11 and S20 (Fig. 1b). In fact, they were both characterized by *Proteobacteria* RAs>70% and shared a rather similar bacterial phylum structure ($B_{11,20} = 0.10$). *Proteobacteria* RAs<54% characterized all the other spring samples.

The within-sample abundance of *Proteobacteria*, *Cyanobacteria*, *Actinobacteria*, *Firmicutes*, and *Bacteroidetes* presented a seasonal trend, since it was on average higher in winter than in spring samples (Fig. S3). In contrast, *Acidobacteria*, *Nitrospirae*, *Armatimonadetes*, *Caldithrix*, and *Spirochaetes* were only found in the spring samples. Each phylum is associated with a main habitat, as shown in Table S3. Consequently, the abundance of the detected phylum's main habitats also showed seasonal variations (Fig. 2a). The overall mean RA of each habitat for the winter and spring samples is also shown in Fig. 2b and c, respectively. Most of the detected bacterial phyla were associated with the terrestrial and aquatic environment (TAE) and the soil (SOI) habitats (Table S3), with an overall relative abundance ~92%. The comparison between Fig. 2b and c shows the seasonal variations of the two most frequent phyla's habitats: TAE and SOI presented a decreasing and

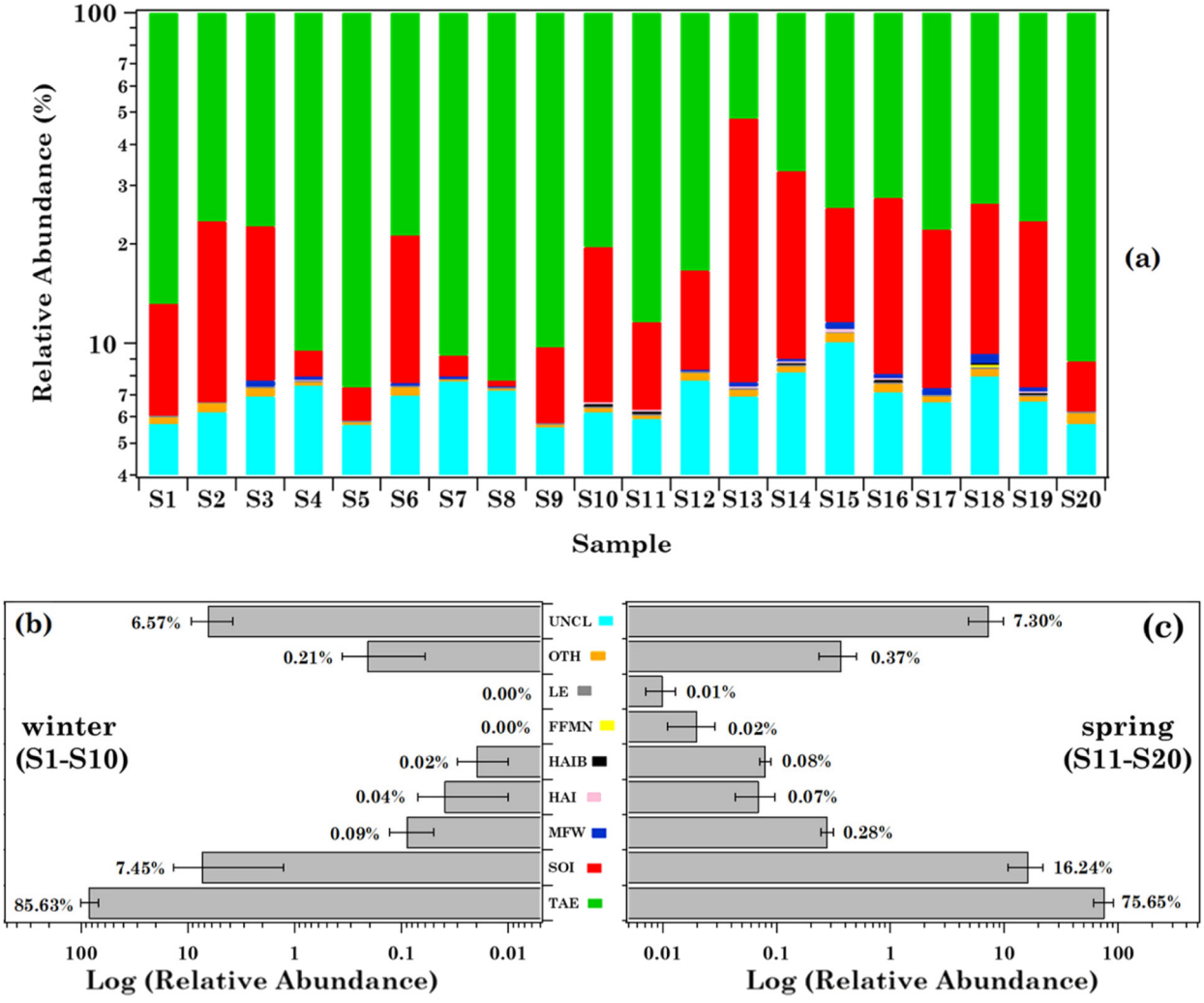

Fig. 2. Percentage contribution (on a logarithmic scale) of the main habitats (terrestrial and aquatic environments TAE; soil SOI; marine and fresh water MFW; human, animal, and insect HAI; host associated-obligate intracellular bacteria HAIB; frequently found in marine niches FFMN; liquid environment LE; other OTH; unclassified UNCL) associated with the identified bacterial phyla: (a) relative contribution in each sample, and mean contribution in (b) winter and (c) spring samples. The error bars in (b) and in (c) represent the standard error of the mean.

increasing trend, respectively, from winter to spring. The lower frequency of rainy days occurring in spring-summer all over the Central Mediterranean Basin favoured the aging of the airborne soil particles and, hence, the increase of the particle contribution from the soil dust source, as outlined in Romano et al. (2020). Therefore, the spring increase of the bacterial phyla associated with the soil habitat (*Actinobacteria*, *Gemmatimonadetes*, *Thermi*, and *Acidobacteria*) was likely favoured by the increase of atmospheric particles associated with the soil dust source. The remaining identified bacterial habitats (marine and fresh water; human, animal, and insect; host associated-obligate intracellular bacteria; frequently found in marine niches; and liquid environment) were characterized by a low overall relative abundance (<0.5%).

3.3. Overview of the RDA triplot

The Redundancy Discriminant Analysis on environmental factors and bacterial phylum abundances was performed to provide a graphical view of the environmental factor-phylum relationships. Chemical species mass concentrations and phylum relative abundances were the predictive and dependent variables, respectively, in this study. Singletons were removed from the RDA, as mentioned.

Fig. 3 shows the RDA triplot relating the microbial composition at the phylum level, PM10 chemical species, and PM10 samples in (a) winter and (b) spring. Red and green arrows indicate environmental factors and response variables, respectively. The arrow length and direction correspond to the variance that can be

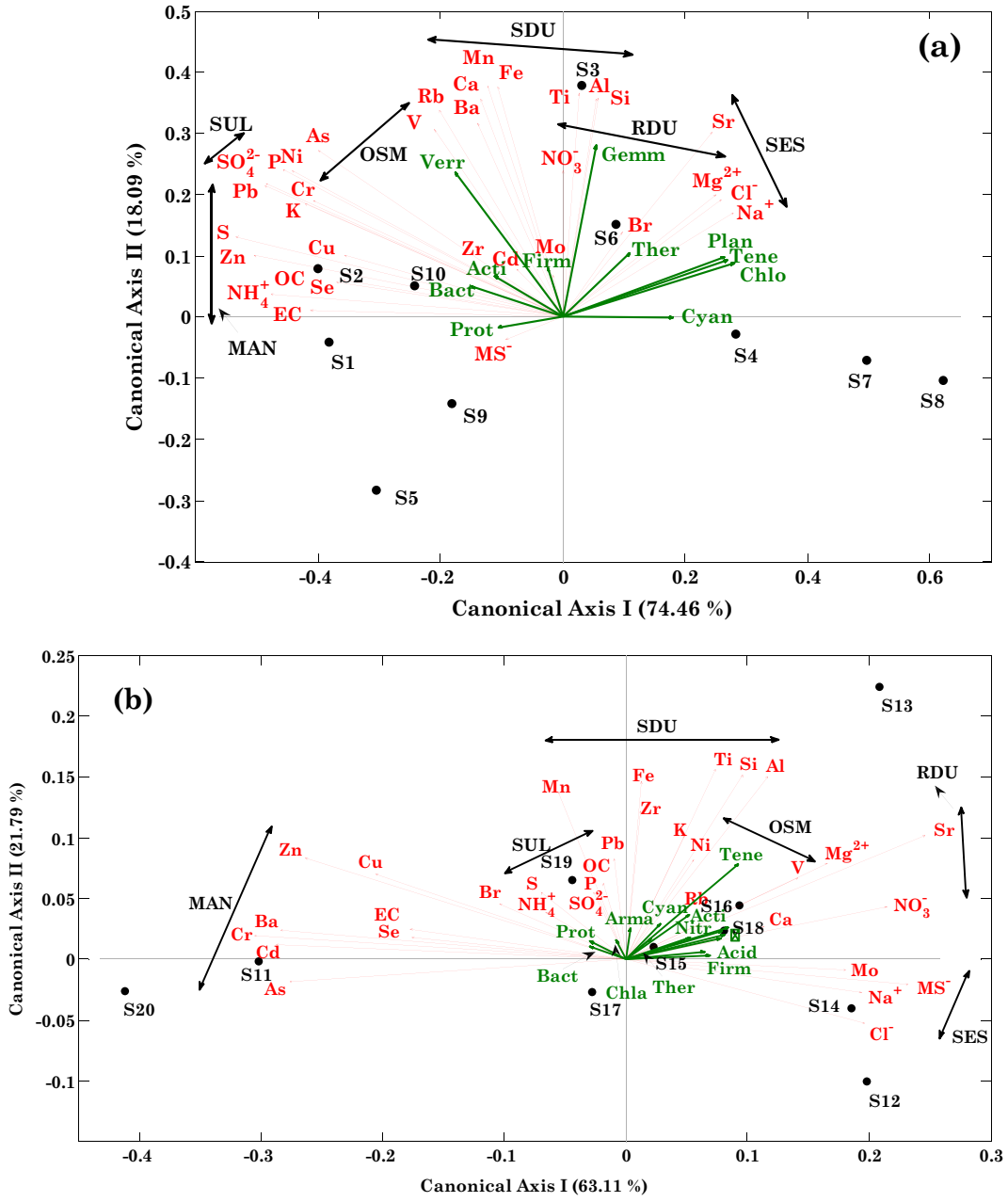

Fig. 3. Ordination plot based on the Redundancy Discriminant Analysis (RDA) between chemical species, the most abundant airborne bacterial phyla (*Proteobacteria* Prot, *Bacteroidetes* Bact, *Actinobacteria* Acti, *Cyanobacteria* Cyan, *Firmicutes* Firm, *Tenericutes* Tene, *Gemmatinomadetes* Gemm, *Verrucomicrobia* Verr, *Chloroflexi* Chlo, *Thermi* Ther, *Planctomycetes* Plan, *Chlamydiae* Chla, *Acidobacteria* Acid, *Nitrospirae* Nitr, and *Armatimonadetes* Arma), and analyzed samples in (a) winter and (b) spring. In (b) β represents Chlo, Plan, Verr, and Gemm. Black arrows indicate the main pollution sources: mixed anthropogenic MAN, sulphate SUL, heavy oils – secondary marine OSM, soil dust SDU, reacted dust RDU, and sea salt SES.

explained by environmental variable and phylum abundance. The greater absolute value of the cosine of the angle between two arrows suggests the stronger correlation between them. An angle close to 90° indicates a weak correlation. The arrow in the same and opposite direction suggests a positive and negative correlation, respectively (e.g., Sun et al., 2018). Fig. 3 shows that the arrows associated with chemical species (red arrows) were on average spread in the canonical axis plane over a wider angle in spring than in winter, suggesting that correlation coefficients between chemical species likely decreased in spring. The spring-summer air mass aging, which favoured the mixing of particles of different type/source (e.g., Romano et al., 2019b), likely contributed to this result. In contrast, bacterial phylum arrows (green arrows) were spread over a wider area of the canonical axis plane in winter than in spring. This last result could likely suggest that the correlation between different phyla on average increased from winter to spring. Phylum arrows were on average smaller in spring (Fig. 3b) than in winter (Fig. 3a) likely because of the smaller value of the explained variance in spring. Fig. 3a and b allowed also identifying clusters of chemical species, which could be associated with different pollution sources according to Table 2. Black double-end arrows in Fig. 3 allowed identifying the main tracers of pollution sources at the study site, according to Perrone et al. (2019a).

Full dots represent winter and spring PM10 samples in Fig. 3a and b, respectively. Two main sample clusters could be identified in winter (Fig. 3a), in accordance with the BC dissimilarity dendrogram of Fig. 1a: the cluster composed by the S3, S4, S6, S7, and S8 samples and the cluster consisting of the S2, S10, S9, S1, and S5 samples. Their location was on average close to the arrow associated with the bacterial phylum that reached the highest abundance in a given sample and/or to the arrow associated with the chemical species that reached the highest mass concentration in that sample. In fact, sample S2 was located rather close to the Zn arrow (Fig. 3a), since Zn reached the highest mass concentration (24 ng m^{-3}) in S2 (Table S1). Sample S3 was rather close to the Ti and Al arrows (Fig. 3a), since they reached the highest mass concentration in that sample (61 and 837 ng m^{-3}, respectively). Moreover, sample S3 was rather close to the arrow associated with the phylum *Gemmatinomadetes*, since it reached the highest RA in S3. Samples S15 and S16 were rather close to the V and Mg^{2+} arrows (Fig. 3b), since V and Mg^{2+} reached one of the highest concentrations in those spring samples. Their location in the RDA triplot of Fig. 3b was also due to the fact that *Tenericutes* and *Cyanobacteria* reached the highest RA in S15 and in S16, respectively.

Other sample sub-clusters could be identified in Fig. 3a, as the one composed by S4, S7, and S8. These last samples were associated with air masses that crossed the Atlantic and the Mediterranean Sea before reaching the study site, according to Romano et al. (2019a). Accordingly, Fig. 3a shows that these samples are close to the arrows related to chemical species identifying particles from the sea salt source. The sub-cluster composed by S1, S2, and S10 was associated with air masses that spent several hours over land or close to the land affected by anthropogenic activities before reaching the study site, according to Romano et al. (2019a). Therefore, Fig. 3a shows that they are rather close to the arrows related to the chemical species associated with the mixed anthropogenic source. The sub-cluster consisting of the samples S3 and S6 was associated with air masses that crossed northern Africa before reaching the study site, according to Romano et al. (2019a). Consequently, Fig. 3a shows that these last samples are close to the arrows related to the chemical species associated with the reacted dust source. Note that the bacterial structure of the samples S3 and S6 is similar to the one of the samples collected by Mescioglu et al. (2019b) over the Northern Red Sea. The lack of *Cyanobacteria* was the main difference between the samples S3 and S6 of this study and the ones collected over the Northern Red Sea. Note that *Cyanobacteria* generally reach high abundances at the study site during the advection of marine air masses (Romano et al., 2019a). Therefore, the lack of *Cyanobacteria* over the Northern Red Sea could be due to the different bacterial structure at the sea surface with respect to the one found over the Mediterranean Sea. However, further studies are required to support this last comment. Observe also that the impact of long-range transported air masses on the chemical speciation of PM samples collected at the study site has been widely reported/ discussed in several previous works (e.g., Perrone et al., 2013a, 2014, 2015).

3.3.1. RDA relationships between chemical species and bacterial phyla in winter and spring samples

The bacterial phylum association with chemical species and, hence, with pollution sources is one of the main outcomes of the RDA triplot and of this study. Fig. 3a indicates that *Chloroflexi*, *Tenericutes*, and *Planctomycetes* were strongly correlated each other, and that were likely associated with chemical species or particles from the sea salt source in winter. *Chloroflexi* and *Planctomycetes* were strongly related to each other and to *Verrucomicrobia*, *Gemmatinomadetes*, and *Thermi* in spring. They were likely associated with chemical species characterizing the reacted dust source (NO_3^- and Mg^{2+}) (Fig. 3b). *Gemmatinomadetes* and *Verrucomicrobia* were likely associated with reacted dust (NO_3^- and Mg^{2+}) and soil dust chemical species (Ca, Fe, Mn, and Ba), respectively, in winter (Fig. 3a). The *Firmicutes* phylum, whose relative abundance was on average twice greater in spring than in winter samples (Fig. 1), was associated with reacted dust and/or sea salt chemical species (NO_3^-, Na^+, Mg^{2+}, and Cl^-) in spring (Fig. 3b) and with soil dust particles (Ca, Fe, Mn, and Ba) in winter (Fig. 3a). *Actinobacteria* was likely associated with chemical species characterizing the heavy oil/secondary marine source (V and Ni) both in winter and in spring. *Bacteroidetes* was likely related to particles from the mixed anthropogenic source (OC, EC, K, and Cu) and/or sulphate source (SO_4^{2-}, NH_4^+, and Pb) both in winter and in spring. *Proteobacteria*, which is the most abundant phylum both in winter and in spring, was likely associated with mixed anthropogenic and/or sulphate chemical species in spring and appeared mainly correlated with mixed anthropogenic chemical species in winter. *Armatimonadetes* and *Chlamydiae* phyla were likely related to particles from the soil dust and/or sulphate source, respectively, in spring.

The comparison of Fig. 3a and b allowed identifying the seasonal changes of the relationships between chemical species/pollution sources and bacterial phyla. In spring, most of the bacterial phyla were associated with chemical species characterizing the heavy oil/secondary marine, reacted dust, and sea salt sources, whose percentage contribution increased from Autumn-Winter to Spring-Summer at the study site, as discussed in Perrone et al. (2019a). The bacterial phylum relative abundances associated with marine and fresh water habitats also increased more than twice from winter to spring (Fig. 2). Therefore, the seasonal changes of chemical species/pollutions sources and the observed relationships may indicate that the main seasonal features of the bacterial community structure were also likely affected by chemical species/pollutions sources.

3.3.2. Chemical species and bacterial phyla relationships by Spearman correlation coefficients and comparison with RDA triplots

The relationships between bacterial phylum relative abundances and chemical species mass concentrations have also been investigated by Spearman correlation coefficients for both winter and spring samples. The goal of the latter analysis was to highlight the relationship strengths, identify main chemical species responsible for the relationships, and compare the results from the correlation coefficient analysis with corresponding RDA results. To this end, singletons, “Other”, and “Unclassified” phyla were removed from the analysis. Tables S4a and S4b show the Spearman correlation coefficients *r*, where values significant at a *p*-level < 0.01 and 0.05 are in bold and in bold-italic, respectively. Table 3 summarizes significant positive and negative relationships between phyla and chemical species for both winter and spring samples.

Table 3
Bacterial phyla positively and negatively correlated with chemical species and other phyla for winter and spring samples. Spearman correlation coefficients are reported in brackets (values significant at a p-level < 0.01 and 0.05 are in bold and in italic, respectively). The arrow indicates the pollution source likely associated with the significantly correlated chemical species.

Bacterial Phyla	Winter		Spring	
	Positive corr.	Negative corr.	Positive corr.	Negative corr.
Proteobacteria (Prot)		Cyan (**−0.82**), Chlo (**−0.78**), Plan (*−0.72*)	Bact (*0.73*)	Acti (*−0.68*), Firm (*−0.71*)
Bacteroidetes (Bact)	As (*0.67*), Ca (**0.77**), SO_4^{2-} (*0.65*), Pb (**0.78**) → **SUL** Acti (**0.76**), Firm (*0.64*)		Cd (*0.73*) → **MAN** Prot (*0.73*)	Cl^- (*0.72*)
Actinobacteria (Acti)	SO_4^{2-} (**0.78**), As (*0.66*), Ba (*0.64*), Pb (*0.65*), V (*0.67*), P (**0.75**), K (*0.71*), Ca (*0.71*), Ti (*0.64*), Mn (**0.78**), Fe (**0.79**), Rb (**0.76**) → **SUL/SDU** Bact (**0.76**), Firm (**0.82**), Verr (*0.68*)	Cyan (*−0.65*)	NO_3^- (*0.66*), Sr (**0.78**) → **OSM** Gemm (*0.70*)	Prot (*−0.68*)
Cyanobacteria (Cyan)	Chlo (*0.72*), Plan (*0.68*)	Cr (*−0.64*), S (*−0.64*) Prot (**−0.82**), Acti (*−0.65*)	Mg^{2+} (**0.82**), Mo (*0.70*) → **SES** Plan (*0.71*)	
Firmicutes (Firm)	SO_4^{2-} (*0.68*), Ti (*0.71*), Mn (*0.71*), Fe (*0.66*) → **SDU** Bact (*0.64*), Acti (**0.82**)		MS^- (*0.66*) → **OSM**	Cr (**−0.83**), Zn (**−0.79**) Prot (*−0.71*)
Tenericutes (Tene)	Plan (*0.67*)	MS^- (**−0.79**)	Nitr (*0.72*)	
Gemmatinomadetes (Gemm)	Na^+ (*0.68*), Mg^{2+} (*0.69*), Cl- (*0.68*), Al (*0.70*), Si (*0.70*), Ti (*0.70*), Sr (*0.70*) → **SDU/SES** Chlo (**0.75**), Plan (**0.75**)		Na^+ (*0.65*), Mg^{2+} (**0.75**), Mo (*0.65*) → **SES** Acid (**0.89**), Acti (*0.70*), Ther (*0.71*)	EC (**−0.76**), P (*−0.64*)
Verrucomicrobia (Verr)	NO_3^- (*0.68*), P (*0.68*), Mn (*0.70*), Fe (*0.70*), Rb (*0.70*) → **SDU/RDU** Acti (*0.68*)		Chlo (*0.72*), Plan (**0.76**), Nitr (*0.64*), Ther (*0.64*)	Ba (*−0.73*)
Chloroflexi (Chlo)	Na^+ (**0.80**), Mg^{2+} (*0.69*), Cl^- (**0.80**), Sr (**0.77**) → **SES** Cyan (*0.72*), Plan (**0.96**), Gemm (**0.75**)	NH_4^+ (**−0.76**) Prot (**−0.78**)	MS^- (**0.83**), Mo (*0.69*), V (*0.67*) → **SES** Verr (*0.72*), Plan (**0.90**)	
Thermi (Ther)			Gemm (*0.71*), Verr (*0.64*)	
Planctomycetes (Plan)	Na^+ (*0.72*), Cl^- (*0.72*), Sr (*0.67*) → **SES** Cyan (*0.68*), Chlo (**0.96**), Gemm (**0.75**), Tene (*0.67*)	NH_4^+ (*−0.65*), MS^- (**−0.74**) Prot (*−0.72*)	Mo (**0.74**) → **SES** Cyan (*0.71*), Chlo (**0.90**), Verr (**0.76**), Nitr (*0.70*)	
Chlamydiae (Chla)				
Acidobacteria (Acid)			Na^+ (**0.82**), Mg^{2+} (**0.77**), Cl^- (*0.72*), Mo (**0.80**) → **SES** Gemm (**0.89**), Arma (*0.64*)	OC (**−0.76**), EC (*0.71*), Cd (*−0.69*), Pb (*−0.71*), P (**−0.84**)
Nitrospirae (Nitr)			Verr (*0.64*), Tene (*0.72*), Plan (*0.70*)	
Armatimonadetes (Arma)			Mg^{2+} (*0.66*), Mo (*0.69*) → **SES** Acid (*0.64*)	

Proteobacteria, the most abundant phylum, does not show any significant positive or negative correlation with chemical species both in winter and in spring, in contrast to RDA results (Fig. 3). *Proteobacteria* was instead negatively correlated with *Cyanobacteria*, *Chloroflexi*, and *Planctomycetes* in W, and with *Actinobacteria* and *Firmicutes* in S, and was positively correlated with *Bacteroidetes* in S, in good accordance with RDA results.

The *Bacteroidetes* phylum was strongly correlated with Ca and Pb and to less extent with SO_4^{2-} and As in winter (Table 3), pointing out its association with the sulphate source. Conversely, in spring, it was positively correlated with Cd indicating its association with the mixed anthropogenic source. These results are in reasonable agreement with corresponding RDA results (Fig. 3).

The significant correlations of *Actinobacteria* with several species from the sulphate and soil dust sources (Table 3) suggested that it was likely associated with particles from both sources in W. This last result was in contrast to the RDA triplot (Fig. 3a), which suggested that *Actinobacteria* was mainly associated with sulphate and/or heavy oil/secondary marine chemical species in W. Both correlation coefficients (Table 3) and RDA triplot (Fig. 3b) suggested that *Actinobacteria* was likely associated with particles from the heavy oil/secondary marine source in S.

The *Cyanobacteria* phylum did not show any significant positive correlation with the analyzed chemical species in W, but it showed significant positive correlation with *Chloroflexi* and *Planctomycetes*. It was strongly correlated with Mg^{2+} and significantly correlated with Mo and *Planctomycetes* in S. These last results were in reasonable agreement with the corresponding RDA triplot (Fig. 3). Molybdenum does not exist naturally in the pure metallic form and is an oligonutrient necessary for many life forms. Table S4 shows that in spring Mo was correlated with Mg^{2+} and Na^+, which are tracers of marine particles (Table 2). Therefore, Mo was likely associated with particles of marine origin in S.

The *Firmicutes* phylum showed positive significant correlations with SO_4^{2-}, Ti, Mn, and Fe and, hence, with soil dust tracers in W, and with MS^- in S, in accordance with corresponding RDA results. The organic anions MS^-, which is a product of the atmospheric oxidation of gaseous dimethylsulfide produced in seawater, is commonly associated with a secondary marine source (Perrone et al., 2019b).

The *Gemmatinomadetes* phylum, which was positively correlated with Na^+, Mg^{2+}, Cl^-, Al, Si, Ti, and Sr (Table 3), was likely associated with soil dust and sea salt tracers in W and with sea salt tracers in S, being associated with Na^+, Mg^{2+}, and Mo, in agreement with RDA results.

Among the less abundant phyla, *Verrucomicrobia* was significantly correlated with NO_3^-, P, Mn, Fe, and Rb (Table 3) and, therefore, it was associated with soil dust and/or reacted dust chemical species in W, in accordance with RDA results (Fig. 3a). *Verrucomicrobia* did not show any significant correlation with chemical species in S, but it was correlated with *Planctomycetes*, *Chloroflexi*, *Nitrospirae*, and *Thermi*, in good accordance with RDA results. The positive correlation with Na^+, Mg^{2+}, Cl^-, and Sr in W and the strong correlation with MS^- in S (Table 3) suggested that *Chloroflexi* was related to sea salt tracers both in W and in S, similarly to RDA results. The *Planctomycetes* phylum, which was correlated with Na^+, Cl^-, and Sr in W and with Mo in S, was likely associated with sea salt chemical species, similarly to what was found by RDA. *Acidobacteria* was related to airborne particles of marine origin in S, because of its positive correlation with Na^+, Mg^{2+}, Cl^-, and Mo, in good accordance with RDA results. *Nitrospirae* did not present any significant correlation with the investigated chemical species. Its positive correlation with *Verrucomicrobia*, *Tenericutes*, and *Planctomycetes* (Table 3) supported its location in the RDA triplot of Fig. 3b. Finally, the *Armatimonadetes* phylum, which was correlated with Mg^{2+} and Mo in S samples, was likely related to particles of marine origin, in contrast to RDA outcomes.

We believe that the results of this section have shown that the correlation coefficients are the best tool to determine relationship strengths and identify main chemical species/pollution sources responsible for the relationships with the collected bacterial phyla. The discrepancies between correlation coefficient results (Table 3) and RDA triplots (Fig. 3) were likely due to the fact that the location of a phylum arrow in the RDA triplot is dependent on more factors (mainly the PM10 sample location, the phylum relationship with other bacteria phyla, and the relationships of bacteria phyla with chemical species) that may be contrasting among them. However, Table 3 showed that the relations of a given phylum with chemical species and other phyla were seasonal dependent, in accordance with RDA results. In fact, the results from Table 3 suggest that most phyla (*Cyanobacteria*, *Firmicutes*, *Gemmatinomadetes*, *Chloroflexi*, *Planctomycetes*, *Acidobacteria*, and *Armatimonadetes*) were mainly correlated with chemical species associated with particles related to the sea salt source only in spring.

3.4. Genera abundance and Bray-Curtis dissimilarity dendrogram in winter and spring samples

Seventy-nine predominant genera, which contributed each by a percentage > 0.01%, were identified in the collected PM10 samples (Romano et al., 2019a). Figs. S4a and S4b show genera heat maps and corresponding BC dissimilarity dendrograms for winter and spring samples, respectively. The corresponding $B_{i,j}$ matrices based on the bacterial genus relative abundances are shown in Table S5. Different clusters of PM10 samples were identified from the BC dissimilarity dendrograms applied to bacterial genera. In winter, we identified the cluster composed by samples S7, S8, S4, S3, and S6, where the genus *Calothrix* reached the highest RAs; the cluster consisting of samples S9 and S10, where the genus *Vibrio* was found; and the cluster composed by S1, S2, and S5, where the genus *Pseudomonas* reached the highest RAs (Fig. S4a). Four main clusters could also be identified in spring (Fig. S4b): the cluster composed by samples S15, S18, S16, S19, S17, and S14, where the genus *Bradyrhizobium* reached the highest RA values; the cluster consisting of samples S11 and S20, with the highest RAs of genus *Pseudomonas*; and finally the clusters composed by sample S12 and by sample S13, where the genus *Bacillus* and the genus *Streptomyces* reached the highest RA, respectively.

The sample clusters identified by the genus BC dissimilarity dendrograms were on average different from the ones obtained by the phylum BC dissimilarity dendrograms (Fig. S3), since the relations with other genera and/or with chemical species could be different from the ones of corresponding phyla.

3.4.1. Relationships between genera and chemical species by Spearman correlation coefficients and RDA triplots

The relationships between bacterial genera relative abundances and between genera abundances and chemical species mass concentrations

Table 4
Most abundant bacterial genera (mean relative abundance >0.6% both in winter and in spring) positively and negatively correlated with chemical species and other genera for winter and spring samples. Spearman correlation coefficients are reported in brackets (values significant at a p-level < 0.01 and 0.05 are in bold and in italic, respectively). The arrow indicates the pollution source likely associated with the significantly correlated chemical species.

Bacterial genera	Winter		Spring	
	Positive correlations	Negative correlations	Positive correlations	Negative correlations
Calothrix (CAL)		Cr (*−0.67*) *PSE* (**−0.83**), *ENT* (*−0.75*)	*SPM* (*0.64*), *MET* (*0.73*)	Cd (*−0.65*) *PSE* (*−0.73*)
Pseudomonas (PSE)	*ENT* (**0.95**)	*CAL* (**−0.83**)	*CHR* (*0.75*), *ENT* (**0.81**), *ARS* (*0.68*), *ACI* (*0.73*)	*CAL* (*−0.73*), *SPM* (**−0.83**)
Bacillus (BAC)	Ti (*0.74*) → **SDU**			Zn (**−0.77**)
Enterobacter (ENT)	*PSE* (**0.95**)	Sr (*−0.70*) *CAL* (*−0.75*)	Cr (**0.77**) → **MAN** *PSE* (**0.81**), *CHR* (**0.87**), *ARS* (**0.84**)	
Streptomyces (STR)		*ACI* (*−0.64*)	*MET* (0.71)	As (*−0.70*)
Sphingomonas (SPM)			Sr (*0.67*) → **SES/SDU** *CAL* (*0.64*), *MET* (**0.81**)	*PSE* (**−0.83**), *ARS* (*−0.68*), *ACI* (**−0.84**)
Hyphomicrobium (HYP)	*MET* (**0.97**)		*MET* (**0.93**)	
Chryseobacterium (CHR)	Cd (**0.77**), Pb (*0.69*) → **MAN** *ARS* (**0.85**)		*ENT* (**0.87**), *ARS* (*0.70*)	
Rickettsia (RIC)		NH_4^+ (*−0.65*), MS^- (**−0.81**)	*MET* (*0.67*)	P (*−0.64*)
Arthrospira (ARS)	*CHR* (**0.85**)		*PSE* (*0.68*), *CHR* (*0.70*), *ENT* (**0.84**), *ACI* (**0.77**)	Mg^{2+} (*−0.68*), Mo (*−0.70*) *SPM* (*−0.68*)
Methyloversatilis (MET)	*HYP* (**0.97**)		*HYP* (**0.93**)	
Acinetobacter (ACI)		V (*−0.72*), Al (*−0.66*), Si (*−0.66*), Ti (*−0.68*), Fe (*−0.64*) *STR* (*−0.64*)	*PSE* (*0.73*), *ARS* (**0.77**)	MS^- (*−0.65*), V (*−0.67*), Ca (*−0.67*), Sr (**−0.83**) *SPM* (**−0.84**), *MET* (*−0.72*)

have firstly been investigated by the Spearman correlation coefficients (Table S6). Tables 4 and S7 summarize the significant positive and negative relationships between the most abundant bacterial genera (with mean RA > 0.6% both in winter and in spring) and chemical species both in winter and in spring. The RDA on environmental factors and bacterial genera restricted to the most abundant genera is shown in Fig. 4, which allowed identifying the clusters of chemical species associated with the main pollution sources at the study site (Table 2). Clusters of PM10 samples could also be identified in Fig. 4, in reasonable accordance with the ones resulting from the BC dissimilarity dendrograms (Fig. S4). In fact, each sample is generally close to the bacterial genus that reached the highest RA in that sample and/or to the chemical species that reached the highest mass percentage in that sample. The genus *Pseudomonas* reached the highest winter RA in the cluster composed by S1 (28.04%), S2 (27.64%), and S5 (36.07%), as shown in Fig. 4a. The highest OC mass concentrations were also reached in samples S1 and S2 (13.2 and 9.0 μg m^{-3}, respectively, Table S1). Sample S10 was associated with particles from the heavy oil/secondary marine source likely because of the high MS^- mass concentration (0.013 μg m^{-3}) in that sample. Samples S7, S8, S4, S3, and S6 were all rather close to the genus *Calothrix*, which reached the highest RAs in those samples, according to Fig. S4a. Moreover, they were rather close to the chemical species associated with the sea salt source because the mass concentration of Na^+, Cl^-, and Mg^{2+} reached high values in those samples.

Environmental factor and genus arrows were spread all over the canonical axis plane both in W and in S, in contrast to the corresponding bacterial phylum results (Fig. 3). Table 4 shows that rather few bacterial genera were significantly and positively correlated with chemical species (unlike the results for the bacterial phyla, Table 3), since most genera were only correlated with other genera. *Calothrix* was correlated with *Sphingomonas* and *Methyloversatilis* and anti-related to Cd and *Pseudomonas* in spring, in accordance with the RDA triplot (Fig. 4b). *Pseudomonas*, *Enterobacter*, *Sphingomonas*, and *Methyloversatilis* are *Proteobacteria* genera,

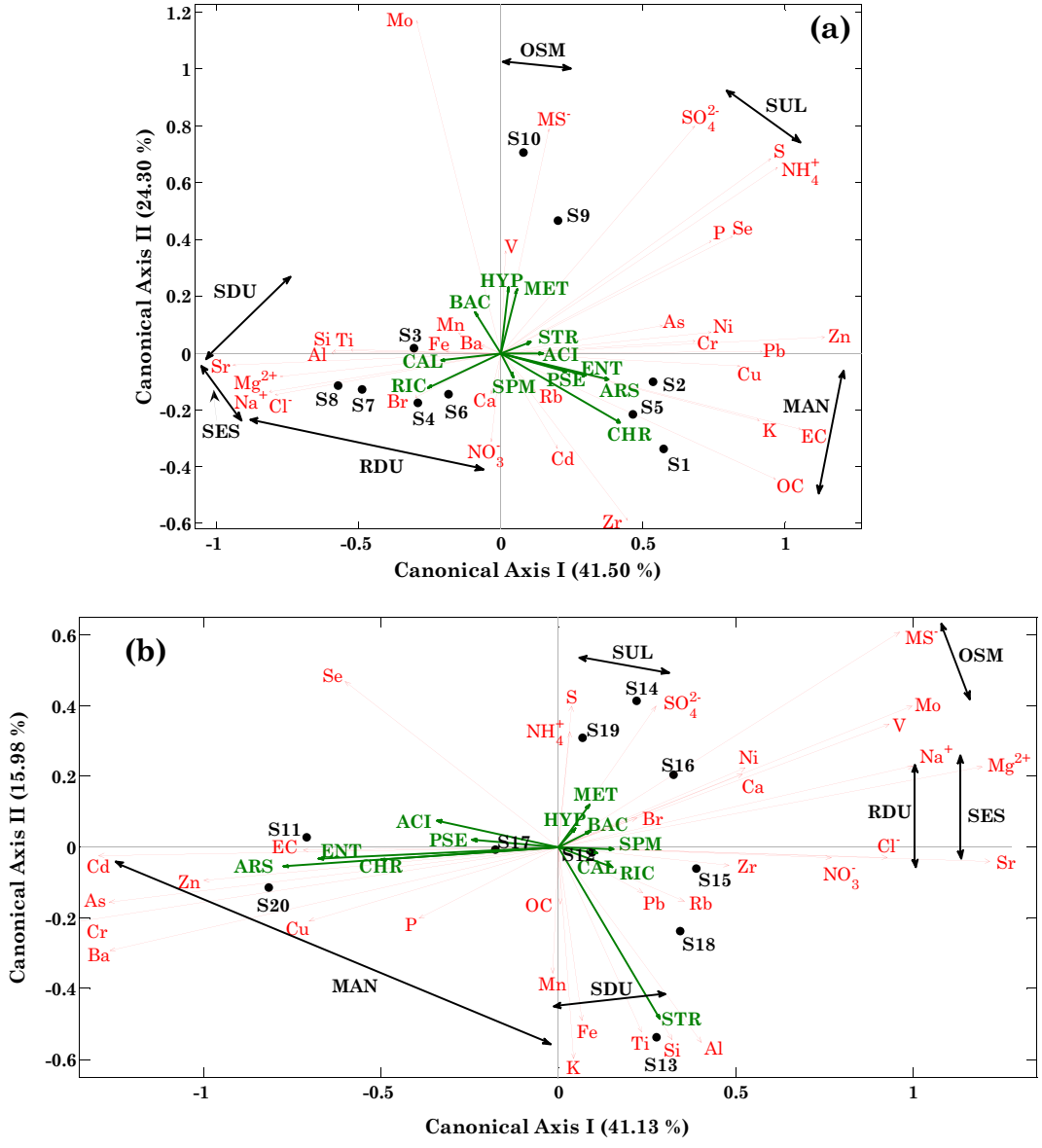

Fig. 4. Ordination plot based on the Redundancy Discriminant Analysis (RDA) between chemical species, the most abundant airborne genera (*Acinetobacter* ACI, *Arthrospira* ARS, *Bacillus* BAC, *Calothrix* CAL, *Chryseobacterium* CHR, *Enterobacter* ENT, *Hyphomicrobium* HYP, *Methyloversatilis* MET, *Pseudomonas* PSE, *Rickettsia* RIC, *Sphingomonas* SPM, *Streptomyces* STR), and analyzed samples in (a) winter and (b) spring. Black arrows indicate the main pollution sources: mixed anthropogenic MAN, sulphate SUL, heavy oils – secondary marine OSM, soil dust SDU, reacted dust RDU, and sea salt SES.

while *Calothrix* is a *Cyanobacteria* genus. Therefore, these last results suggest that the correlation between genera may not be dependent on the associated phyla.

In winter, *Bacillus* was significantly correlated with Ti ($r = 0.74$, Table 4) and weakly correlated with Mn, Al, and Si ($r = 0.61$, Table S6a). Therefore, it was likely associated with chemical species characterizing the soil dust source, in reasonable agreement with the RDA triplot (Fig. 4a). *Bacillus* is a genus belonging to the *Firmicutes* phylum that was also associated with soil dust particles in winter (Table 3 and Fig. 3a). In spring, the genus *Bacillus* was anti-related only to Zn, conversely the corresponding phylum *Firmicutes* was significantly correlated only with MS^-. The genus *Enterobacter* was significantly anti-related to Sr and *Calothrix*, and positively correlated with *Pseudomonas* in W, while it was significantly correlated with Cr ($r = 0.77$) and weakly correlated with Cu ($r = 0.59$), Cd ($r = 0.59$), and Ba ($r = 0.59$) in S (Table S6b). Therefore, it was likely associated with mixed anthropogenic chemical species in S, in good accordance with RDA outcomes (Fig. 4b). *Sphingomonas* did not show any significant correlation with chemical species and bacterial genera in winter (Table 4). It was significantly correlated with Sr and weakly correlated with Fe, Mn, Al, Si, Ti, and Rb in spring. Therefore, it was likely associated with sea salt and/or soil dust chemical species in S, in accordance with RDA outcomes.

The relationships between bacterial genera RAs and between genera RAs and chemical species mass concentrations on average varied with seasons, as shown in Table 4 and Fig. 4. However, RDA triplots indicated significant correlations for all tested bacterial genera with other genera and/or with chemical species. In contrast, the Spearman correlation coefficient analysis (Table 4) showed that only few genera were significantly correlated with chemical species.

3.4.2. Comparison with results from other studies

In this subsection, the RDA results of this work are compared with the corresponding ones from previous studies, to better show the dependence of RDA outcomes on the monitoring site features and geographical location. As mentioned, some previous studies analyzed the relationships between the bacterial structure and the PM chemical composition by RDA plots. Guo et al. (2018) investigated the biological and chemical composition of atmospheric PM during haze days in Beijing (China) and found that *Sphingomonas*, *Methyloversatilis*, and *Acinetobacter* were negatively correlated with OC. In contrast, the RDA triplots of this study showed that *Sphingomonas*, *Methyloversatilis*, and *Acinetobacter* were weakly correlated with OC both in winter and in spring (Fig. 4a and b, respectively). Sun et al. (2018) investigated the correlation of the bacterial community with chemical components in atmospheric PM spring samples in Beijing. They found that *Pseudomonas* was weakly correlated with NH_4^+ and that *Sphingomonas* and *Bacillus* were positively correlated with SO_4^{2-}, Na^+, K^+, Mg^{2+}, Ca^{2+}, and OC, in reasonable accordance with the results of this study (see Fig. 4b). Zhong et al. (2019) also investigated by RDA plots the relationships between chemical components and airborne bacterial genera in winter PM2.5 samples collected in Guilin (southwestern China). They found that *Pseudomonas*, *Sphingomonas*, and *Bacillus* were within the ten most abundant genera, in good accordance with the results of this study. Moreover, they found that *Pseudomonas*, *Sphingomonas*, and *Bacillus* assumed negative correlation with Mg^{2+} and positive correlations with SO_4^{2-}, NO_3^-, NH_4^+, Na^+, K^+, and Cl^-, which were associated with particles mainly produced from vehicle exhaust and fuel combustion. The positive correlations of *Sphingomonas* and *Bacillus* with SO_4^{2-}, NO_3^-, NH_4^+, Na^+, and Cl^- are in reasonable accordance with the one of this study mainly in spring (Fig. 4b), while *Pseudomonas* was mainly associated with particles from the mixed anthropogenic source at the study site (Fig. 4). Innocente et al. (2017) found from PM samples collected in Milan (Italy) that *Sphingomonas* was correlated with Ca^{2+}, in accordance with the results of this study. In particular, they explained that this last relation could suggest a common origin of both *Sphingomonas* and $Ca^{2+\text{from soil}}$. In fact, research activities on the relationships between the airborne bacterial community structure and the chemical species/pollution sources may be important to better investigate about the main processes/carriers responsible for the bacterial diffusion within the atmosphere.

In conclusion, we have observed that the correlations between bacterial genera abundances and chemical species mass concentrations could vary from site to site, being dependent on PM fraction, seasons, and monitoring site features. However, some common relationships can be observed worldwide, mainly for the most abundant bacteria.

4. Conclusion

The relationships between the airborne bacterial community structure both at the phylum and at the genus level and the chemical composition of winter and spring PM10 samples have been investigated in this study by Redundancy Discriminant Analysis and Spearman correlation coefficients.

- Chemical species were associated with the six main pollution sources (mixed anthropogenic, sulphate, heavy oil/secondary marine, soil dust, reacted dust, and sea salt) identified at the study site by the Positive Matrix Factorization technique to highlight the relationships between bacterial community structure and pollution sources.
- The RDA triplots based on the mass concentration of chemical species and phylum relative abundances highlighted the winter-spring changes of the relationships between phyla and chemical species/pollution sources. *Proteobacteria*, the most abundant phylum, which was correlated with *Bacteroidetes* both in winter and in spring, was mainly associated with chemical species from the mixed anthropogenic source (OC, EC, Cu, and Ba) and/or the sulphate source (SO_4^{2-} and NH_4^+) in spring and with mixed anthropogenic chemical species (OC, EC, and Cu) in winter. *Cyanobacteria*, the second most abundant phylum in winter, which was correlated with *Chloroflexi* and *Planctomycetes*, was mainly correlated with chemical species from the sea salt source (Na^+, Cl^-, and Mg^{2+}) in winter and from the soil dust source (Al, Si, Ti, and Sr) and the heavy/oil secondary marine source (Ni and V) in spring.
- Spearman correlation coefficients also showed that the phylum relationships with chemical species and/or other phyla varied with seasons, in accordance with RDA outcomes. However, we found that on average each phylum showed significant correlations with a smaller number of chemical species and/or other phyla and a few contrasting results.
- Analogously to phylum results, RDA triplots and Spearman correlation coefficients also showed that the genera relationships with chemical species and/or other genera varied with seasons. RDA triplots showed significant associations of all tested bacterial genera with other genera and/or with chemical species. In contrast, few bacterial genera were significantly and positively correlated with chemical species and/or other genera, according to the Spearman correlation coefficients. *Calothrix* and *Pseudomonas,* the most abundant genera, did not show any significant positive correlation with chemical species both in winter and in spring, in contrast to RDA outcomes.
- The contrasting results between correlation coefficients and RDA outcomes were likely due to the fact that the phylum/genus and chemical species location in RDA triplots was also dependent on the PM10 sample location in the graphical framework. In fact, each PM10 sample was on average close to the chemical species and/or the phylum/genus that reached the highest mass concentration or relative abundance, respectively, in that sample.
- Therefore, Spearman correlation coefficients were likely the best tool to determine relationship strengths and obtain unequivocal identifications of the correlations between phyla/genera and chemical species/pollution sources, according to the above comments.
- The comparison of RDA outcomes and correlation coefficients may

represent a significant topic addressed by this work, since results from previous studies were mainly based on RDA plots.
- We also found that the correlation between different genera was not dependent on the corresponding phyla.

In conclusion, correlation analyses between phyla/genera and chemical species from filter-collected atmospheric particles may be rather important, since they can contribute to the research activities on the main diffusion and transport paths of bacteria within the atmosphere. More specifically, strong correlations between phyla/genera and chemical species may indicate the main pollution sources responsible for airborne bacteria dispersion/transport within the atmosphere.

CREDIT AUTHOR STATEMENT.

S.R. and M.R.P. conceived, designed, and wrote the manuscript. G.R. collected the PM10 samples. S.B. and F.L. performed ion chromatography and PIXE analyses, respectively, on the PM10 samples. All authors approved the manuscript.

Declaration of competing interest

The authors declare that they have no known competing financial interests or personal relationships that could have appeared to influence the work reported in this paper.

Acknowledgments

S. Romano has carried out this work with the support of a Temporary Researcher position financed by the Italian "*Programma Operativo Nazionale (PON) Ricerca e Innovazione 2014-2020 (Azione I.2 - Attrazione e Mobilità dei Ricercatori)*". The work was partially supported by the PON project "PER-ACTRIS-IT - *Potenziamento della componente italiana dell'Infrastruttura di Ricerca Aerosol, Clouds and Trace Gases Research Infrastructure*" and by the Italian INFN (Istituto Nazionale Fisica Nucleare), in the frame of the project TRACCIA (*Time Resolved Aerosol Characterization: Challenging Improvements and Ambitions*). Professors P. Alifano and A. Talà from Department of Biological and Environmental Sciences and Technologies (University of Salento, Lecce, Italy) are kindly acknowledged for their support on the bacterial community characterization.

Appendix A. Supplementary data

Supplementary data to this article can be found online at https://doi.org/10.1016/j.scitotenv.2020.138899.

References

Barberán, A., Ladau, J., Leff, J.W., Pollard, K.S., Menninger, H.L., Dunn, R.R., Fierer, N., 2015. Continental-scale distributions of dust-associated bacteria and fungi. Proc. Natl. Acad. Sci. U. S. A. 112 (18), 5756–5761. https://doi.org/10.1073/pnas.1420815112.

Becagli, S., Sferlazzo, D.M., Pace, G., di Sarra, A., Bommarito, C., Calzolai, G., Ghedini, C., Lucarelli, F., Meloni, D., Monteleone, F., Severi, M., Traversi, R., Udisti, R., 2012. Evidence for heavy fuel oil combustion aerosols from chemical analyses at the island of Lampedusa: a possible large role of ships emissions in the Mediterranean. Atmos. Chem. Phys. 12, 3479–3492. https://doi.org/10.5194/acp-12-3479-2012.

Birch, M.E., Cary, R.A., 1996. Elemental carbon-based method for monitoring occupational exposures to particulate diesel exhaust. Aerosol Sci. Technol. 25, 221–241. https://doi.org/10.1080/02786829608965393.

Burton, N.C., Grinshpun, S.A., Reponen, T., 2007. Physical collection efficiency of filter materials for bacteria and viruses. Ann. Occup. Hyg. 51 (2), 143–151. https://doi.org/10.1093/annhyg/mel073.

Cao, C., Jiang, W., Wang, B., Fang, J., Lang, J., Tian, G., Jiang, J., Zhu, T.F., 2014. Inhalable microorganisms in Beijing's PM2.5 and PM10 pollutants during a severe smog event. Environ. Sci. Technol. 48 (3), 1499–1507. https://doi.org/10.1021/es4048472.

Cavalli, F., Viana, M., Yttri, K.E., Genberg, J., Putaud, J., 2010. Toward a standardised thermal-optical protocol for measuring atmospheric organic and elemental carbon: the EUSAAR protocol. Atmos. Meas. Tech. 3, 79–89. https://doi.org/10.5194/amt-3-79-2010.

Chow, J.C., 1995. Critical review: measurement methods to determine compliance of ambient air quality standards for suspended particles. J. Air Waste Manage. Assoc. 45, 320–385. https://doi.org/10.1080/10473289.1995.10467369.

Edgar, R.C., 2013. UPARSE: highly accurate OTU sequences from microbial amplicon reads. Nat. Methods 10, 996–998. https://doi.org/10.1038/nmeth.2604.

Estillore, A.D., Trueblood, J.V., Grassian, V.H., 2016. Atmospheric chemistry of bioaerosols: heterogeneous and multiphase reactions with atmospheric oxidants and other trace gases. Chem. Sci. 7, 6604. https://doi.org/10.1039/c6sc02353c.

Fröhlich-Nowoisky, J., Kampf, C.J., Weber, B., Huffman, J.A., Pöhlker, C., Andreae, M.O., Lang-Yona, N., Burrows, S.M., Gunthe, S.S., Elbert, W., Su, H., Hoor, P., Thines, E., Hoffmann, T., Després, V.R., Pöschl, U., 2016. Bioaerosols in the earth system: climate, health, and ecosystem interactions. Atmos. Res. 182, 346–376. https://doi.org/10.1016/j.atmosres.2016.07.018.

Ganesan, A., Oates, T., Schmill, M., 2016. Finding Representative Points in Multivariate Data Using PCA. ArXiv Preprint (arXiv: 1610.05819).

Gao, J.F., Fan, X.Y., Li, H.Y., Pan, K.L., 2017. Airborne bacterial communities of PM2.5 in Beijing-Tianjin-Hebei megalopolis, China as revealed by Illumina MiSeq sequencing: a case study. Aerosol Air Qual. Res. 17, 788e798. https://doi.org/10.4209/aaqr.2016.02.0087.

Gat, D., Mazar, Y., Cytryn, E., Rudich, Y., 2017. Origin-dependent variations in the atmospheric microbiome community in Eastern Mediterranean Dust Storms. Environ. Sci. Technol. 51, 6709–6718. https://doi.org/10.1021/acs.est.7b00362.

Guo, Z., Wang, Z., Qian, L., Zhao, Z., Zhang, C., Fu, Y., Li, J., Zhang, C., Lu, B., Qian, J., 2018. Biological and chemical compositions of atmospheric particulate matter during hazardous haze days in Beijing. Environ. Sci. Pollut. Res. 25, 34540–34549. https://doi.org/10.1007/s11356-018-3355-6.

Herut, B., Rahav, E., Tsagaraki, T.M., Giannakourou, A., Tsiola, A., Psarra, S., Lagaria, A., Papageorgiou, N., Mihalopoulos, N., Theodosi, C.N., Violaki, K., Stathopoulou, E., Scoullos, M., Krom, M.D., Stockdale, A., Shi, Z., Berman-Frank, I., Meador, T.B., Tanaka, T., Paraskevi, P., 2016. The potential impact of Saharan dust and polluted aerosols on microbial populations in the East Mediterranean Sea, an overview of a Mesocosm experimental approach. Front. Mar. Sci. 3, 226. https://doi.org/10.3389/fmars.2016.00226.

Hiraoka, S., Miyahara, M., Fujii, K., Machiyama, A., Iwasaki, W., 2017. Seasonal analysis of microbial communities in precipitation in the greater Tokyo area, Japan. Front. Microbiol. 8, 1506. https://doi.org/10.3389/fmicb.2017.01506.

Innocente, E., Squizzato, S., Visin, F., Facca, C., Rampazzo, G., Bertolini, V., Gandolfi, I., Franzetti, A., Ambrosini, R., Bestetti, G., 2017. Influence of seasonality, air mass origin and particulate matter chemical composition on airborne bacterial community structure in the Po Valley, Italy. Sci. Total Environ. 593–594, 677–687. https://doi.org/10.1016/j.scitotenv.2017.03.199.

Jones, D.L., 2017. Fathom Toolbox for MATLAB: software for multivariate ecological and oceanographic data analysis. College of Marine Science, University of South Florida, St. Petersburg, FL, USA https://www.marine.usf.edu/research/matlab-resources/.

Jordaan, K., Bezuidenhout, C.C., 2016. Bacterial community composition of an urban river in the north west Province, South Africa, in relation to physico-chemical water quality. Environ. Sci. Pollut. Res. 23, 5868–5880. https://doi.org/10.1007/s11356-015-5786-7.

Katra, I., Arotsker, L., Krasnov, H., Zaritsky, A., Kushmaro, A., Ben-Dov, E., 2014. Richness and diversity in dust Stormborne biomes at the southeast Mediterranean. Sci. Rep. 4, 5265. https://doi.org/10.1038/srep05265.

Kellogg, C.A., Griffin, D.W., 2006. Aerobiology and the global transport of desert dust. Trends Ecol. Evol. 21 (11), 638–644. https://doi.org/10.1016/j.tree.2006.07.004.

Legendre, P., Gallagher, E.D., 2001. Ecologically meaningful transformations for ordination of species data. Oecologia 129, 271–280. https://doi.org/10.1007/s004420100716.

Li, W., Yang, J., Zhang, D., Li, B., Wang, E., Yuan, H., 2018. Concentration and community of airborne bacteria in response to cyclical haze events during the fall and midwinter in Beijing, China. Front. Microbiol. 9, 1741. https://doi.org/10.3389/fmicb.2018.01741.

Lucarelli, F., Nava, S., Calzolai, G., Chiari, M., Udisti, R., Marino, F., 2011. Is PIXE still a useful technique for the analysis of atmospheric aerosols? The LABEC experience. X-Ray Spectrom. 40, 162–167. https://doi.org/10.1002/xrs.1312.

Mackey, K.R.M., Buck, K.N., Casey, J.R., Cid, A., Lomas, M.W., Sohrin, Y., Paytan, A., 2012. Phytoplankton responses to atmospheric metal deposition in the coastal and open-ocean Sargasso Sea. Front. Microbiol. 3, 1–15. https://doi.org/10.3389/fmicb.2012.00359.

Mayol, E., Jimenez, M.A., Herndl, G.J., Duarte, C.M., Arrieta, J.M., 2014. Resolving the abundance and air-sea fluxes of airborne microorganisms in the North Atlantic Ocean. Front. Microbiol. 5, 557. https://doi.org/10.3389/fmicb.2014.00557.

Mayol, E., Arrieta, J.M., Jiménez, M.A., Martínez-Asensio, A., Garcias-Bonet, N., Dachs, J., González-Gaya, B., Royer, S.J., Benítez-Barrios, V.M., Fraile-Nuez, E., et al., 2017. Long-range transport of airborne microbes over the global tropical and subtropical ocean. Nat. Commun. 8, 1–8. https://doi.org/10.1038/s41467-017-00110-9.

Mazar, Y., Cytryn, E., Erel, Y., Rudich, Y., 2016. Effect of dust storms on the atmospheric microbiome in the eastern Mediterranean. Environ. Sci. Technol. 50 (8), 4194–4202. https://doi.org/10.1021/acs.est.5b06348.

Mescioglu, E., Rahav, E., Belkin, N., Xian, P., Eizenga, J.M., Vichik, A., Herut, B., Paytan, A., 2019a. Aerosol microbiome over the Mediterranean Sea diversity and abundance. Atmosphere 10, 440. https://doi.org/10.3390/atmos10080440.

Mescioglu, E., Rahav, E., Frada, M.J., Rosenfeld, S., Raveh, O., Galletti, Y., Santinelli, C., Herut, B., Paytan, A., 2019b. Dust-associated airborne microbes affect primary and bacterial production rates, and eukaryotes diversity, in the northern Red Sea: a Mesocosm approach. Atmosphere 10, 358. https://doi.org/10.3390/atmos10070358.

Morganti, A., Becagli, S., Castellano, E., Severi, M., Traversi, R., Udisti, R., 2007. An improved flow analysis-ion chromatography method for determination of cationic and anionic species at trace levels in Antarctic ice cores. Anal. Chim. Acta 603, 190–198. https://doi.org/10.1016/j.aca.2007.09.050.

Mykytczuk, N.C., Wilhelm, R.C., Whyte, L.G., 2012. *Planococcus halocryophilus* sp. nov., an extreme sub-zero species from high Arctic permafrost. Int. J. Syst. Evol. Microbiol. 62 (8), 1937–1944. https://doi.org/10.1099/ijs.0.035782-0.

Paliy, O., Shankar, V., 2016. Application of multivariate statistical techniques in microbial ecology. Mol. Ecol. 25 (5), 1032–1057. https://doi.org/10.1111/mec.13536.
Pan, Y., Pan, X., Xiao, H., Xiao, H., 2019. Structural characteristics and functional implications of PM2.5 bacterial communities during fall in Beijing and Shanghai, China. Front. Microbiol. 10, 2369. https://doi.org/10.3389/fmicb.2019.02369.
Perrone, M., Becagli, S., Garcia Orza, J.A.G., Vecchi, R., Dinoi, A., Udisti, R., Cabello, M., 2013a. The impact of long-range-transport on PM1 and PM2.5 at a Central Mediterranean site. Atmos. Environ. 71, 176–186. https://doi.org/10.1016/j.atmosenv.2013.02.006.
Perrone, M.R., Carofalo, I., Dinoi, A., Buccolieri, A., Buccolieri, G., 2009. Ionic and elemental composition of TSP, PM10, and PM2.5 samples collected over south-east Italy. Il Nuovo Cimento B 124, 341–356. https://doi.org/10.1393/ncb/i2009-10770-2.
Perrone, M.R., Piazzalunga, A., Prato, M., Carofalo, I., 2011. Composition of fine and coarse particles in a coastal site of the central Mediterranean: carbonaceous species contributions. Atmos. Environ. 45 (39), 7470–7477. https://doi.org/10.1016/j.atmosenv.2011.04.030.
Perrone, M.R., Dinoi, A., Becagli, S., Udisti, R., 2013b. Chemical composition of PM1 and PM2.5 at a suburban site in southern Italy. Int. J. Environ. An. Ch. 94, 127–150. https://doi.org/10.1080/03067319.2013.791978.
Perrone, M.R., Romano, S., Orza, J.A.G., 2014. Particle optical properties at a Central Mediterranean site: impact of advection routes and local meteorology. Atmos. Res. 145–146, 152–167. https://doi.org/10.1016/j.atmosres.2014.03.029.
Perrone, M.R., Romano, S., Orza, J.A.G., 2015. Columnar and ground-level aerosol optical properties: sensitivity to the transboundary pollution, daily and weekly patterns, and relationships. Environ. Sci. Pollut. R. 22, 16570–16589. https://doi.org/10.1007/s11356-015-4850-7.
Perrone, M.R., Romano, S., Genga, A., Paladini, F., 2018. Integration of optical and chemical parameters to improve the particulate matter characterization. Atmos. Res. 205, 93–106. https://doi.org/10.1016/j.atmosres.2018.02.015.
Perrone, M.R., Vecchi, R., Romano, S., Becagli, S., Traversi, R., Paladini, F., 2019a. Weekly cycle assessment of PM mass concentrations and sources, and impacts on temperature and wind speed in southern Italy. Atmos. Res. 218, 129–144. https://doi.org/10.1016/j.atmosres.2018.11.013.
Perrone, M.R., Bertoli, I., Romano, S., Russo, M., Rispoli, G., Pietrogrande, M.C., 2019b. PM2.5 and PM10 oxidative potential at a Central Mediterranean site: contrasts between dithiothreitol- and ascorbic acid-measured values in relation with particle size and chemical composition. Atmos. Environ. 210, 143–155. https://doi.org/10.1016/j.atmosenv.2019.04.047.
Peter, H., Hörtnagl, P., Reche, I., Sommaruga, R., 2014. Bacterial diversity and composition during rain events with and without Saharan dust influence reaching a high mountain lake in the Alps. Environ. Microbiol. Rep. 6 (6), 618–624. https://doi.org/10.1111/1758-2229.12175.
Pietrogrande, M.C., Manarini, F., Perrone, M.R., Udisti, R., Romano, S., Becagli, S., 2018. PM10 oxidative potential at a central Mediterranean site: association with chemical composition and meteorological parameters. Atmos. Environ. 188, 97–111. https://doi.org/10.1016/j.atmosenv.2018.06.013.
Polymenakou, P.N., Mandalakis, M., Stephanou, E.G., Tselepides, A., 2008. Particle size distribution of airborne microorganisms and pathogens during an intense African dust event in the eastern Mediterranean. Environ. Health Perspect. 116 (3), 292–296. https://doi.org/10.1289/ehp.10684.
Querol, X., Alastuey, A., Pey, J., Cusack, M., Pérez, N., Mihalopoulos, N., Theodosi, C., Gerasopoulos, E., Kubilay, N., Koçak, M., 2009. Variability in regional background aerosols within the Mediterranean. Atmos. Chem. Phys. 9, 4575–4591. https://doi.org/10.5194/acp-9-4575-2009.
Rahav, E., Ovadia, G., Paytan, A., Herut, B., 2016. Contribution of airborne microbes to bacterial production and N_2 fixation in seawater upon aerosol deposition. Geophys. Res. Lett. 43. https://doi.org/10.1002/2015GL066898.
Rahav, E., Paytan, A., Mescioglu, E., Galletti, Y., Rosenfeld, S., Raveh, O., Santinelli, C., Ho, T.-Y., Herut, B., 2018a. Airborne microbes contribute to N_2 fixation in surface water of the northern Red Sea. Geophys. Res. Lett. 45. https://doi.org/10.1029/2018GL077132.
Rahav, E., Belkin, N., Paytan, A., Herut, B., 2018b. Phytoplankton and bacterial response to desert dust deposition in the coastal waters of the southeastern Mediterranean sea: a four-year in situ survey. Atmosphere 9, 305. https://doi.org/10.3390/atmos9080305.
Rahav, E., Belkin, N., Paytan, A., Herut, B., 2019. The relationship between air-mass trajectories and the abundance of dust-borne prokaryotes at the SE Mediterranean Sea. Atmosphere 10, 280. https://doi.org/10.3390/atmos10050280.
Raisi, L., Aleksandropoulou, V., Lazaridis, M., Katsivela, E., 2013. Size distribution of viable, cultivable, airborne microbes and their relationship to particulate matter concentrations and meteorological conditions in a Mediterranean site. Aerobiologia 29, 233–248. https://doi.org/10.1007/s10453-012-9276-9.
Reche, I., D'Orta, G., Mladenov, N., Winget, D.M., Suttle, C.A., 2018. Deposition rates of viruses and bacteria above the atmospheric boundary layer. ISME J 12, 1154–1162. https://doi.org/10.1038/s41 396-017-0042-4.
Ricotta, C., Podani, J., 2017. On some properties of the Bray-Curtis dissimilarity and their ecological meaning. Ecol. Complex. 31, 201–205. https://doi.org/10.1016/j.ecocom.2017.07.003.
Romano, S., Di Salvo, M., Rispoli, G., Alifano, P., Perrone, M.R., Talà, A., 2019a. Airborne bacteria in the central Mediterranean: structure and role of meteorology and air mass transport. Sci. Total Environ. 697, 134020. https://doi.org/10.1016/j.scitotenv.2019.134020.
Romano, S., Perrone, M.R., Pavese, G., Esposito, F., Calvello, M., 2019b. Optical properties of PM2.5 particles: results from a monitoring campaign in southeastern Italy. Atmos. Environ. 203, 35–47. https://doi.org/10.1016/j.atmosenv.2019.01.037.
Romano, S., Perrone, M.R., Becagli, S., Pietrogrande, M.C., Russo, M., Caricato, R., Lionetto, G., 2020. Ecotoxicity, genotoxicity, and oxidative potential tests of atmospheric PM10 particles. Atmos. Environ. 221, 117085. https://doi.org/10.1016/j.atmosenv.2019.117085.
Seinfeld, J.H., Pandis, S.N., 1998. Atmospheric Chemistry and Physics: From Air Pollution to Climate Change. J. Wiley &Sons, INC.
Sharoni, S., Trainic, M., Schatz, D., Lehahn, Y., Flores, M.J., Bidle, K.D., Ben-Dor, S., Rudich, Y., Koren, I., Vardi, A., 2015. Infection of phytoplankton by aerosolized marine viruses. Proc. Natl. Acad. Sci. U. S. A. 112 (21), 6643–6647. https://doi.org/10.1073/pnas.1423667112.
Sun, Y., Xu, S., Zheng, D., Li, J., Tian, H., Wang, Y., 2018. Effects of haze pollution on microbial community changes and correlation with chemical components in atmospheric particulate matter. Sci. Total Environ. 637–638, 507–516. https://doi.org/10.1016/j.scitotenv.2018.04.203.
Van Den Wollenberg, A.L., 1977. Redundancy analysis: an alternative for canonical correlation analysis. Psychometrika 42, 207. https://doi.org/10.1007/BF02294050.
Viana, M., Kuhlbusch, T.A.J., Querol, X., Alastuey, A., Harrison, R.M., Hopke, P.K., Winiwarter, W., Vallius, M., Szidat, S., Prévôt, A.S.H., Hueglin, C., Bloemen, H., Wåhlin, P., Vecchi, R., Miranda, A.I., Kasper-Giebl, A., Maenhaut, W., Hitzenberger, R., 2008. Source apportionment of PM in Europe: a review of methods and results. J. Aerosol Sci. 39, 827–849. https://doi.org/10.1016/j.jaerosci.2008.05.007.
Wang, T., Cai, G., Qiu, Y., Fei, N., Zhang, M., Pang, X., Jia, W., Cai, S., Zhao, L., 2012. Structural segregation of gut microbiota between colorectal cancer patients and healthy volunteers. ISME J 6, 320–329. https://doi.org/10.1038/ismej.2011.109.
Wei, K., Zheng, Y., Li, J., Shen, F., Zou, Z., Fan, H., Li, X., Wu, C.Y., Yao, M., 2015. Microbial aerosol characteristics in highly polluted and near-pristine environments featuring different climatic conditions. Sci. Bull. 60, 1439–1447. https://doi.org/10.1007/s11434-015-0868-y.
Yahya, R.Z., Arrieta, J.M., Cusack, M., Duarte, C.M., 2019. Airborne prokaryote and virus abundance over the Red Sea. Front. Microbiol. 10, 1112. https://doi.org/10.3389/fmicb.2019.01112.
Yan, D., Zhang, T., Su, J., Zhao, L.-L., Wang, H., Fang, X.-M., Zhang, Y.-Q., Liu, H.-Y., Yu, L.-Y., 2018. Structural variation in the bacterial community associated with airborne particulate matter in Beijing, China, during hazy and non-hazy days. Appl. Environ. Microbiol. 84, e00004–e00018. https://doi.org/10.1128/AEM.00004-18.
Zhai, Y., Li, X., Wang, T., Wang, B., Li, C., Zeng, G., 2018. A review on airborne microorganisms in particulate matters: composition, characteristics and influence factors. Environ. Int. 113, 74–90. https://doi.org/10.1016/j.envint.2018.01.007.
Zhen, Q., Deng, Y., Wang, Y., Wang, X., Zhang, H., Sun, X., et al., 2017. Meteorological factors had more impact on airborne bacterial communities than air pollutants. Sci. Total Environ. 60, 703–712. https://doi.org/10.1016/j.scitotenv.2017.05.049.
Zhong, S., Zhang, L., Jiang, X., Gao, P., 2019. Comparison of chemical composition and airborne bacterial community structure in PM2.5 during haze and non-haze days in the winter in Guilin, China. Sci. Total Environ. 655, 202–210. https://doi.org/10.1016/j.scitotenv.2018.11.268.